

University Children's Hospital Ulm  
Head: Prof. Dr. Klaus-Michael Debatin

# **In vitro effect of ionizing radiation on primary glioblastoma cells as a basis for multitarget therapy**

To obtain the doctoral degree of Medicine at the Medical Faculty of Ulm University

Sebastian Haßlacher  
Ravensburg

2019



Acting Dean: Prof. Dr. Thomas Wirth  
1st reviewer: Prof. Dr. Klaus-Michael Debatin  
2nd reviewer: Prof. Dr. Georg Karpel-Massler  
Day of graduation: 12.12.2019



Parts of this work have been published in:

Grunert M., Kassubek R., Danz B., Klemenz B., **Hasslacher S.**, Stroh S., Schneelee L., Langhans J., Ströbele S., Barry S.E., Zhou S., Debatin K.M., Westhoff M.A., **Radiation and Brain Tumors: An Overview.** *Critical Reviews in Oncogenesis*, 23:119-138 (2018)

and:

**Hasslacher S.**, Schneelee L., Stroh S., Langhans J., Zeiler K., Patricia K., Karpel-Massler G., Siegelin M., Schneider M., Zhou S., Grunert M., Halatsch ME., Nonnenmacher L., Debatin K.M., Westhoff M.A. **Inhibition of PI3K signalling increases the efficiency of radiotherapy in glioblastoma cells.** *International Journal of Oncology*, 53:1881-1896 (2018)



# Contents

<b>List of Abbreviations</b>	<b>v</b>
<b>1 Introduction</b>	<b>1</b>
1.1 Cancer . . . . .	1
1.2 Glioblastoma - a brain cancer . . . . .	2
1.3 Therapy methods for glioblastoma . . . . .	2
1.4 Aim of this work . . . . .	9
<b>2 Material and Methods</b>	<b>10</b>
2.1 Material . . . . .	10
2.2 Methods . . . . .	15
<b>3 Results</b>	<b>22</b>
3.1 Effects of irradiation on glioblastoma cells . . . . .	22
3.2 Multitarget chemotherapy in combination with ionizing radiation on glioblastoma cells . . . . .	35
<b>4 Discussion</b>	<b>40</b>
4.1 Effects of irradiation on glioblastoma cells . . . . .	40
4.2 RIST/aRIST as multitarget chemotherapy for G35dif and U87MG . . . . .	47
4.3 Effects of multitarget therapy with ionizing radiation for G35dif . . . . .	48
<b>5 Summary</b>	<b>51</b>
<b>6 Bibliography</b>	<b>52</b>
<b>Acknowledgements</b>	<b>66</b>
<b>Curriculum vitae</b>	<b>67</b>



## **List of Abbreviations**

<b>APS</b>	Ammoniumpersulfate
<b>aRIST</b>	alternative RIST
<b>ATM</b>	Ataxia Telangiectasia Mutated
<b>BCA</b>	Bicinchoninic acid
<b>BRCA 2</b>	Breast Cancer Associated 2
<b>BSA</b>	Bovine serum albumine
<b>DDR</b>	DNA Damage Response
<b>DMEM</b>	Dulbecco's modified Eagle's medium
<b>DMEM/F12</b>	Dulbecco's modified Eagle's medium F12
<b>DMSO</b>	Dimethyl sulfoxide
<b>DNA-PKcs</b>	DNA-dependent protein kinase, catalytic subunit
<b>DSB</b>	double-strand breaks
<b>DTT</b>	Dithiothreitol
<b>EDTA</b>	Ethylenediaminetetraacetic acid
<b>EGF</b>	epidermal growth factor
<b>EGFR</b>	epidermal growth factor receptor
<b>FCS</b>	Fetal calf serum
<b>FD-IR</b>	Fractionated Dose Irradiation
<b>FGF</b>	fibroblast growth factor
<b>FGFR</b>	fibroblast growth factor receptor
<b>HEPES</b>	2-[4-(2-hydroxyethyl)piperazin-1-yl]ethanesulfonic acid
<b>HNSCC</b>	Head and Neck Squamous Cell Carcinoma



## *Contents*

<b>HCL</b>	Hydrogen chloride
<b>HRR</b>	Homologous Recombination Repair
<b>IR</b>	ionizing radiation
<b>MGMT</b>	O6 Methylguanine methyltransferase
<b>mTOR</b>	Mammalian target of rapamycin
<b>NHEJ</b>	non-homologous end joining
<b>PBS</b>	Phosphate Buffered Saline
<b>PI</b>	Propidium iodide
<b>PIP<sub>3</sub></b>	Phosphatidylinositol-trisphosphate
<b>PI3K</b>	Phosphatidylinositol 3 Phosphat Kinase
<b>RIST</b>	Rapamycin, Irinotecan, Sunitinib, Temozolomide
<b>ROS</b>	Reactive oxygen species
<b>RTK</b>	Receptor Tyrosin Kinase
<b>SD-IR</b>	Single Dose Irradiation
<b>SDS</b>	Sodium Dodecyl Sulfate
<b>SF</b>	Survival Fraction
<b>TEMED</b>	Tetramethylethylenediamine
<b>TIC</b>	Tumor Initiating Cells
<b>TRIS</b>	Tris(hydroxymethyl)-aminomethane
<b>VEGFR</b>	Vasoendothelial Growth Factor Receptor
<b>GDC/S</b>	GDC-0941/Sunitinib
<b>R/S</b>	Rapamycin/Sunitinib
<b>I/T</b>	SN-38/Temozolomide



# 1 Introduction

## 1.1 Cancer

Cancer is a term used for neoplastic diseases, in which cells leave their physiological role as "servants" of a greater organism. The exact interaction of organized cellular proliferation and death, as well as the strict fulfillment of its purpose by every cell is a fundamental requirement for homeostasis of higher organisms. Cancer arises from an imbalance between cellular growth and cellular death and is characterized by the hallmarks of cancer, which namely are: 1) evasion of apoptosis 2) self-sufficiency in growth signals 3) insensitivity to anti-growth signals 4) tissue invasion and metastasis 5) limitless replicative potential 6) sustained angiogenesis 7) deregulation of cellular energetics 8) avoiding of immune destruction 9) tumor-promoting inflammation and 10) genomic instability and mutation [42] [43]. Each of these characteristics can be considered as a criteria for the tumor's malignancy but also as a possible target for cancer therapy. Of course, not every hallmark is present in every cancer and depending on tissue and location, cancer is a generic term for a variety of heterogeneous diseases. Cancer becomes symptomatic, as soon as neoplastic cells interfere with physiological homeostasis. This happens for example by endocrine secretion, immunologic disturbances and pain or organ failure by the uncontrolled growth of tumor cells. Cancer treatment aims to maximize quantity and quality of life by the enduring reduction of tumor mass and the best possible re-installation of physiological homeostasis. Therapy currently consists of surgery, radiotherapy and chemotherapy as the three mainstays of treatment. According to the diversity of the disease, therapies are adapted to the tumor's individual characteristics.



## 1.2 Glioblastoma - a brain cancer

The diagnosis of glioblastoma, also known as glioblastoma multiforme (GBM), is still one of the most frightened diagnosis in medicine today. Although the average age at diagnosis is 59 years, unfortunately brain tumors are quite common among children, making up 23% of all childhood tumors in Germany [78] [53]. For adults, glioblastoma is the most frequent primary brain tumor, accounting for more than 70% among all neoplasms of the central nervous system [108] and develop de novo in 95% of cases [77]. While brain tumors corrupt the organ that defines us as a person, life quality is highly compromised among those afflicted [61]. Due to limited space inside the skull, the tumor mass raises intracranial pressure, leading to progressive loss of consciousness, seizures, paralysis like dysphagia and other neurological deficits [96]. Untreated, patients typically die within 3 months, as the tumor grows rapidly with multifocal micro-metastatic spread [111]. According to the Stupp regimen, glioblastoma is currently treated with surgical excision followed by radiotherapy in combination with DNA-alkylating temozolomide. "Radiotherapy is applied as fractionated focal irradiation in daily fractions of 2Gy, given 5 days per week for 6 weeks, for a total of 60Gy" [98]. Simultaneously, temozolomide is given 7 days per week during irradiation and thereafter, if the tumor is therapy respondent. Because of its diffuse growth, with micrometastasis all over the brain, glioblastoma always evades complete surgical excision and intracranial localization prohibits radical neurosurgery. Consequently, patients have poor outcomes with an average survival of 14 months [98]. Under these circumstances, new therapeutic options and research about the nature of this tumor are needed. In this context, predictive preclinical models are important as a basis to create reliable new treatment regimens.

## 1.3 Therapy methods for glioblastoma

### 1.3.1 Killing the cancer cell: Damage, Repair and Death

The traditional concept of radio-chemotherapy is the induction of tumor cell death by cellular stress and damage, which exceeds the capacities of cellular repair. As illustrated



in Fig.1, inducers of cellular stress can be extremely diverse [106]. On a molecular level, DNA is the most vulnerable target and DNA Damage Response (DDR) is the corresponding cellular reaction.

Here, stabilization of p53 protein, a short half-life tetramer, is the key reaction. p53 gets stabilized by phosphorylation of ATM, ATR and DNA-PK, as illustrated in Fig.1, and acts as a transcription factor for pro-apoptotic proteins like Bax, Bad or Bid and p21 which affects cell cycle arrest. As an end point, cells either die (e.g. by apoptosis) or recover and p53 levels normalize again.

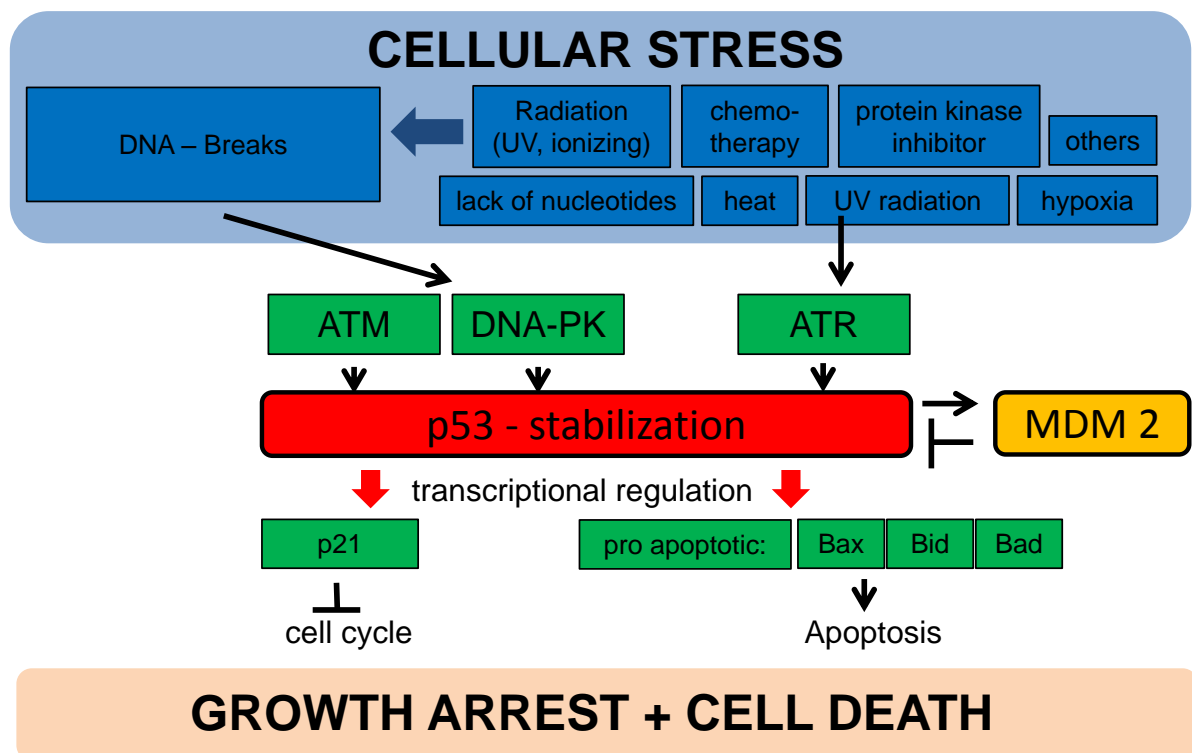


**Figure 1** – Cellular stress leads to cell cycle arrest and cell death through p53 activation. ATM = Ataxia telangiectasia mutated; DNA-PK = DNA Protein Kinase; ATR = Ataxia telangiectasia and Rad3 related; Graphic on the basis of Vogelstein et al. [103] and Weinberg R. [106] p.316

### Repair of DNA double strand breaks (DSB)

Among DNA damage, double-strand breaks (DSB) are most dangerous and lethal for the cell as they lead to chromosomal mismatches. Therefore, repair of these lesions is essential for the cell and different repair mechanisms are available depending on cell cycle



## 1 Introduction

position in the cell cycle [101]: In S and G2 phase, as cells are doubling or have already doubled their DNA content, homologous sister chromatin strands serve as a template for disrupted strands. This repair is called **Homologous Recombination Repair (HRR)**, but it is dependent on the prevalence of a complete (G2 phase) or partial (S-phase) sister chromatin. Independent from the prevalence of sister chromatin strands, **Non Homologous End Joining (NHEJ)** takes effect in G1, S and G2 phase.

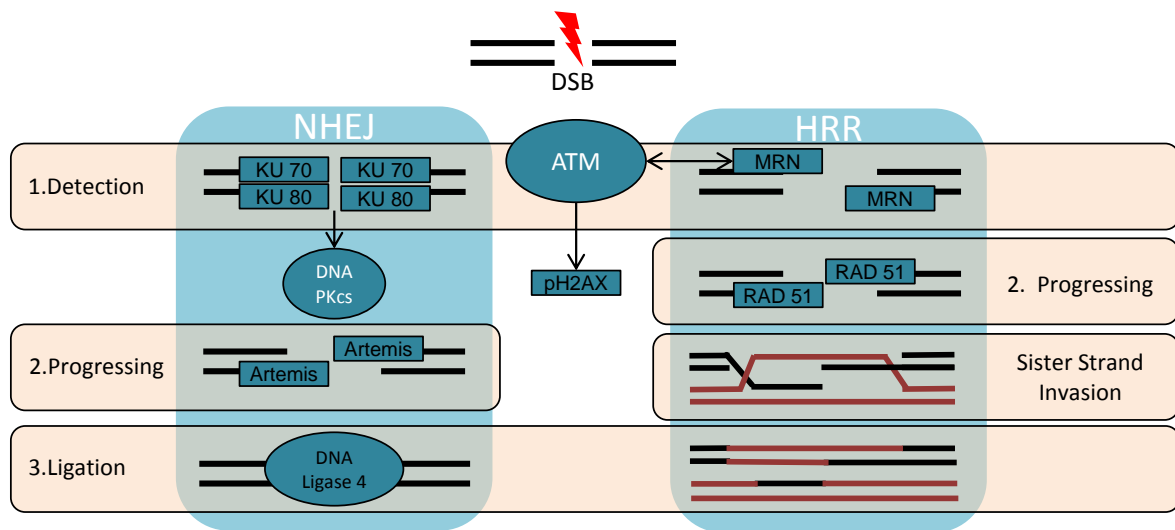


**Figure 2** – Basic steps of Non homologous endjoining (NHEJ) and Homologous Recombination Repair (HRR) after DNA double strand breaks (DSB). ATM = Ataxia Telangiectasia Mutated; MRN=Mre11/Rad50/Nbs1; pH2AX=phosphorylated Histon A2

The initial events after DNA-DSB and their exact chronology are still under investigation but occur most likely simultaneously and can not be put into a define temporal order [101]. Figure 2 displays a rough chronology and the differences in NHEJ and HRR. Basic principals in DNA damage repair are: first the detection and end recognition of DNA Damage, second the recruitment of progressing proteins and third the syntheses and ligation of DNA strands. Among the first events is the decondensation of chromatin and the poly ADP ribosylation (PAR) by Poly ADP ribose polymerases (PARP) [62]. PARP also ribosylates Ataxia Telangiectasia Mutated (ATM), a central player in DNA damage response. This activation is central as ATM phosphorylates various substrates, notably Histon H2 (H2AX) which can be visualized by immunohistochemical staining and p53, the central player for cell cycle arrest [93]. In NHEJ DNA breaking sites are detected by the



binding of Ku70/80 heterodimer [65]. Ku then leads to an activation of DNA-dependent protein kinase, catalytic subunit (DNA-PKcs), a member of the PIK3-kinase family. This step is KU-dependent and essential for NHEJ [65]. Proceeding NHEJ, Artemis, an endonuclease, which defect leads to severe combined immune deficiency (SCID) is taken into duty [64]. Finally, DNA ligation is accomplished by DNA ligase IV (LIG4) [76]. For HRR, DNA breaking sites are tagged by the MRN (NBS, MRE11, Rad50s) complex which is specific for HRR [59]. The Breast Cancer Associated 2 (BRCA 2) protein leads to the attachment of Rad51, which promotes sister strand invasion before finally the defects are resynthesised by DNA ligase [76].

### Cell death and Apoptosis

A cell can be considered "dead" either by losing the integrity of its plasma membrane, by fragmentation of its DNA into apoptotic bodies or in vivo by the engulfment by another cell [56]. Cell death is referred to **Necrosis**, if cells gain cellular volume (oncosis) with swelling of organelles until rupture of their plasma membrane with subsequent loss of intracellular content [56]. Thereby factors are released which induce an immunologic response with local inflammation [36]. Often, necrosis is a result of a sudden breakdown in energy supply (e.g. by disruption of cellular contents by radioactive rays), which can be reproduced experimentally by impairing cellular ATP production [116]. For diagnosis of glioblastoma, necrotic tissues is mandatory in pathologic examination.

In addition, the cell has a physiologic cell death program called **Apoptosis**, which is the regulator for cell number in the human body. Via death receptors (namely FAS, DR4, DR5 TNFR1 and DR3), the **extrinsic apoptotic program** is activated by the initiation of a death-inducing signaling complex (DISC) which leads to procaspase 8 and 10 cleavage. These initiator caspases activate the executioner caspases 3, 6 and 7 which start fragmentation of cellular proteins. Cleavage of structural proteins and unloading of DNase, leads to nuclear shrinkage and DNA fragmentation resulting in morphological characteristic apoptotic bodies with an intact plasma membrane [106] [24]. It is accompanied by retraction of pseudopodes, reduction of cellular volume (pyknosis) and the



engulfment by resident phagocytes in vivo without inflammation [56].

Furthermore, cells have an **intrinsic apoptotic program** which is based on the balance of pro-apoptotic (for example Bad, Bid, Bax) and antiapoptotic proteins (for example Bcl2) which control channels in the outer mitochondrial membrane. In case of high cellular damage, the balance between cellular surviving and death signals might turn out in favor of the latter. If pro-apoptotic channel opening predominates, the mitochondrial membrane depolarizes and cytochrome c leaks out into cytoplasm [48]. There, cytochrome c associates with Apaf-1, forming a hexamer called apoptosome, which cleaves and activates procaspase 9. Caspase 9 then activates executioner caspases 3,6 and 7 and the apoptotic cascade is activated as described.

As tumor cells try to evade this program, which is a hallmark of malignancy, sensitizing and reinduction of apoptosis is a major aim in tumor treatment.

### 1.3.2 Ionizing Radiation (IR)

Ionizing radiation is a well-known tumor treatment and has been used clinically directly after its discovery in 1896 [11]. It is still the most effective therapy for glioma and, therefore, part of the therapy scheme [7]. Although the radiation process itself is a very short termed process, the biological effects on the cell and the united cell structure are complex and go beyond the time of irradiation. The molecular effects of IR are primary cell damage, either **directly** by disruption of cellular structures (DNA, proteins, lipid layers) or **indirectly** by radiolysis of water meaning the generation of especially Reactive oxygen species (ROS) and reactive nitrogen species (RNS) ( $e_{aq}^-$ ,  $H^+$ ,  $OH^-$ ,  $H_2$ ,  $H_2O_2$ ,  $H^+$ ,  $O_2^-$ , etc.) [40]. In addition to initial direct effects, IR also leads to a longlasting cellular damage, even to the cells' progeny [80] [97], due to enhanced ROS leakage from mitochondria, which is the richest natural source of ROS [5] [15]. Still, oxygen is one of the most effective radio sensitizers and reoxygenation between IR - fractions can increase cellular damage [40]. Today, radiotherapy is delivered focally due to precise imaging in order to reduce side effects on healthy tissues. In glioblastoma treatment, IR is applied as Fractionated Dose Irradiation (FD-IR), with 2Gy fractions every 24 hours five times per week [98].



### 1.3.3 Chemotherapy

Classical chemotherapy generally interferes with DNA replication leading to strand breaks in order to take effect on fast dividing tumor cells. The term "classical" is used here in contrast to modern "specific" inhibitors, which selectively target aberrant (e.g. overexpressed) cellular receptors or pathways.

**Temozolomide** is an alkylating agent of DNA and currently the standard chemotherapeutic for glioblastoma treatment. By adding a methyl group to guanine, temozolomide leads to a base mismatch during DNA replication, which triggers a DNA repair response, cell cycle arrest and finally, if the amount of damage exceeds a certain level, apoptosis [89]. The latter is dependent on the amount of DNA methylation. As cells can remove the methyl group by O6 Methylguanine methyltransferase (MGMT) the MGMT status of tumor cells is critical for therapy response [47].

In addition, **Irinotecan** is used in this work for combination therapy with temozolomide. Its active metabolite SN-38 inhibits topoisomerase I and prevents DNA from uncoiling. Thereby it inhibits translation and replication and leads to DNA strand breaks and cell death. Though, combination therapy of irinotecan and temozolomide alone has proven rather disappointing results in clinical studies [81].

### 1.3.4 Targeting aberrant signalling: Specific Inhibitors and Multitarget Therapy

New insights in tumor biology revealed aberrant signaling pathways as new target for chemotherapy. Frequent genetic alteration of 88% in the RTK/RAS/PI3K pathway in GBM revealed it as a promising target for specific therapy [70]. The RTK/RAS/PI3K pathway is associated with protein synthesis, cell cycle progression and proliferation (see Fig.3). Growth Factor Receptors are activated by substrates like epidermal growth factor receptor (EGFR), Vasoendothelial Growth Factor Receptor (VEGFR) or fibroblast growth factor receptor (FGFR) leading to activation of cytoplasmic kinase activity. This can be inhibited by **Sunitinib**, an inhibitor of Receptor Tyrosin Kinase (RTK). Subsequently, RTK activates Phosphatidylinositol 3 Phosphatase Kinase (PI3K), which generates



## 1 Introduction

PIP<sub>3</sub> as a second messenger. PI3K can be inhibited by **Pictilisib (GDC-0941)**. Further signal transmission goes to AKT (syn. Protein Kinase B), which affects various substrates [87]. This includes inhibition of pro-apoptotic proteins like Bad and Mammalian target of rapamycin (mTOR), which activates protein synthesis via phosphorylation of ribosomal protein S6. mTOR is inhibited via **Rapamycin** (syn. Sirolimus).

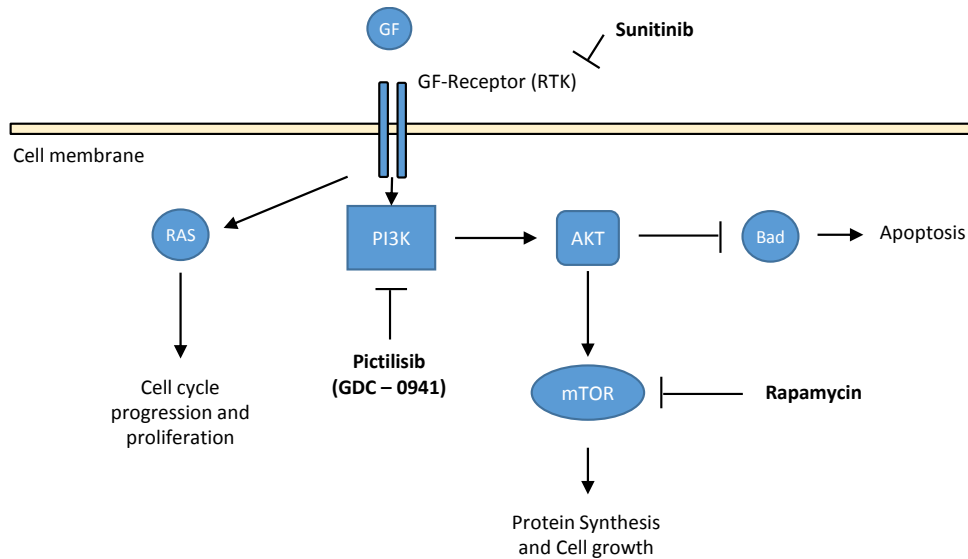


**Figure 3 – Overview of RTK/PI3K/mTOR signalling** Growth factors (GF) like EGFR activate RTK receptors on the cell surface, which transmit the signal to intracellular PI3K. PI3K phosphorylates Phosphatidylinositol-trisphosphate (PIP<sub>3</sub>) as a second messenger, which activates AKT. Active AKT has various substrates, including inhibition of pro-apoptotic proteins (e.g. Bad) and mTOR, an activator of protein synthesis via phosphorylation of ribosomal S6. In addition RTK signalling also activates Ras signalling, activating cell cycle progression and proliferation. EGFR = Endothelial Growth Factor Receptor, RTK = Receptor Tyrosin Kinase, PIP<sub>3</sub> = Phosphatidylinositol-trisphosphate, mTOR = mammalian target of Rapamycin

Although RTK/PI3K/mTOR pathway plays an important role in tumor progression [13], single pathway inhibition by the use of sunitinib or rapamycin alone have not been successful in clinical trials [79] [2]. However, combination therapy with new specific pathway inhibitors with classical chemotherapeutics in multitarget therapy schemes is a promising new approach.



### 1.3.5 Multitarget Therapy: RIST and aRIST

Multitarget therapy aims on the intelligent combination of classical chemotherapy with specific substances which target cellular signaling. On this basis it is possible to re-instate cellular susceptibility to cell death (e.g. apoptosis) or boost cell damage from chemotherapy avoiding high dose chemotherapy. For glioblastoma, the "**RIST**"-therapy has shown remarkable potential in preclinical and clinical application [75]. "RIST" is an acronym for the four agents: **R**apamycin, **I**rinotecan, **S**unitinib and **T**emozolomide. Clinically, RIST therapy is applied as a two weeks' interval scheme with a weekly alteration of classical chemotherapeutics (temozolomide and irinotecan) and specific inhibitors (rapamycin and sunitinib). Currently, RIST therapy is available for compassionate use in glioblastoma and refractory neuroblastoma as a relatively well-tolerated chemotherapy [75].

## 1.4 Aim of this work

Multitarget therapy is a promising new approach in cancer treatment. As radiotherapy is a well-established glioblastoma treatment, interaction of IR with multitarget therapy schemes like RIST is of interest. First, because patients receiving RIST therapy for compassionate use have already undergone radiotherapy and second, because radiotherapy as standard point of care is always part for further clinical trials. In addition, radiotherapy is a promising component for new multitarget therapy schemes itself. Therefore the knowledge about molecular effects and timing of this method is crucial for its implementation.

The aim of this work was the establishment of an in vitro irradiation protocol for primary differentiated glioblastoma cells to serve as a basis for combinatory multitarget radiochemotherapy. In order to get reliable predictions for clinical settings, the protocol should mimic the clinical situation regarding dose and timing best possible. In a second step, this protocol was applied to multitarget RIST therapy.



## 2 Material and Methods

### 2.1 Material

#### 2.1.1 Antibodies

Antibody	Corporation and Location
Mouse anti- $\gamma$ H2AX	Millipore, Temecula, USA
Goat anti-mouse	Millipore, Temecula, USA
Mouse anti-p21	BD Bioscience, Heidelberg, Germany
Mouse anti-p53	BD Bioscience, Heidelberg, Germany
Mouse anti-Ku70	Abcam, Cambridge, UK
Mouse anti-Ku80	Abcam, Cambridge, UK
Mouse anti-AKT	BD Bioscience, Heidelberg, Germany
Mouse anti-S6	Cell Signaling, Frankfurt, Germany
Rabbit anti-pAKT(Ser473)	Cell Signaling, Frankfurt, Germany
Rabbit anti-pS6	Cell Signaling, Frankfurt, Germany
Mouse anti-CyclinD1	Life Technologies, Carlsbad, USA
Mouse anti $\beta$ -aktin	Sigma, Hamburg, Germany
Goat anti-mouse	Santa Cruz Biotec, Dallas, USA
Goat anti-rabbit	Santa Cruz Biotec, Dallas, USA
Mouse anti-cyclinD1	Life technologies, Carlsbad, USA

#### 2.1.2 Biomaterials

##### Primary cultures of glioblastoma

Glioblastoma Tumor Initiating Cells (TIC) were isolated from surgical specimens and primary glioblastoma cells were derived as described in section 2.2.1. The study was



## 2 Material and Methods

approved by the Ethics Committee, Medical Faculty, Ulm University (Antrag 162/10).

Name	Histology	Age	Sex
TIC G35	WHO IV glioma	44	m
TIC G38	WHO IV glioma	75	m

### Industrial cell lines

Cell line	Corporation and Location
U87MG ATCC	ATCC LGC Standard, Teddington, UK

### 2.1.3 Chemicals and Reagents

#### Medium reagents

Reagent	Corporation and Location
Dulbecco's modified Eagle's medium (DMEM)	Invitrogen, Waltham, USA
Dulbecco's modified Eagle's medium F12 (DMEM/F12)	Invitrogen, Waltham, USA
Fetal calf serum (FCS)	Invitrogen, Waltham, USA
L-Glutamin	Invitrogen, Waltham, USA
2-[4-(2-hydroxyethyl)piperazin-1-yl]ethanesulfonic acid (HEPES)-Buffer	BiochromAG, Berlin, Germany
Fungizone (Amphotericin B)	Invitrogen, Waltham, USA
PenStrep (penicillin/streptomycin)	Invitrogen, Waltham, USA
fibroblast growth factor (FGF)	MACS Milteny Biotec, Gladbach, Germany
epidermal growth factor (EGF)	Biomol GmbH, Hamburg, Germany
B27	Invitrogen, Waltham, USA



### Chemicals and Reagents

Reagent	Corporation and Location
Trypsin/Ethylenediaminetetraacetic acid (EDTA)	Biochrom AG, Berlin, Germany
Phosphate Buffered Saline (PBS)-Dulbecco	Biochrom AG, Berlin, Germany
Trisodium citrate	Fluka, Hamburg, Germany
Propidium iodide (PI)	Sigma, Hamburg, Germany
Bovine Serum Albumine (BSA)	BD Bioscience, Heidelberg, Germany
Paraformaldehyde	Pharmacy Kinderklinik, Ulm, Germany
Triton X 100	Sigma, Hamburg, Germany
CASYton solution	Roche, Mannheim, Germany
Vectashield®MountMedium	Vector Laboratories, Burlingame, USA
FACSFlow™	BD Bioscience, Heidelberg, Germany
Tris(hydroxymethyl)-aminomethane (TRIS)	Trizmabase, Hamburg, Germany
Sodium chloride	Prolabo, Darmstadt, Germany
Glycerol	Roth, Karlsruhe, Germany
Pierce Bicinchoninic acid (BCA) Protein Assay Reagent A	Thermo, Schwerte, Germany
Pierce BCA Protein Assay Reagent B	Thermo, Schwerte, Germany
Pierce Western Blotting Kit	Thermo, Schwerte, Germany
Water (H <sub>2</sub> O)	Ampuwa, Bad Homburg, Germany
30% Acrylamide Mix (30% Acrylamide 0,8% Bisacrylamide(5:1))	Roth, Karlsruhe, Germany
Sodium Dodecyl Sulfate (SDS)	Serva, Heidelberg, Germany
Ammoniumpersulfate (APS)	Merck, Darmstadt, Germany
Tetramethylethylenediamine (TEMED)	BioRad, Munich, Germany
Dithiothreitol (DTT)	Merck, Darmstadt, Germany
Bromphenolblue	Fluka Chemie AG, Buchs, Switzerland
Silicone Paste	GE Bayer, Leverkusen, Germany



## 2 Material and Methods

Dimethyl sulfoxide (DMSO)	Merck, Darmstadt, Germany
Bovine serum albumine (BSA)	Serva, Heidelberg, Germany
Sodium azide	Merck, Darmstadt, Germany
Luminol	Sigma, Hamburg, Germany
Hydrogen Peroxide (H <sub>2</sub> O <sub>2</sub> )	Merck, Darmstadt, Germany
Trisodium citrate dihydrate	Merck, Darmstadt, Germany
Hydrogen chloride (HCL)	Riedel-de Haen, Seelze, Germany
Tween 20 (Polysorbate 20)	Sigma, Hamburg, Germany
Ascorbic acid	Merck, Darmstadt, Germany

### Chemotherapeutics

Reagent	Corporation and Location
Rapamycin	Sigma-Aldrich, Hamburg, Germany
Temozolomide	Schering, Weimar, Germany
Sunitinib	LC Laboratories, Hamburg, Germany
GDC-0941	Genentech, San Francisco, USA
SN-38	Tocris, Wiesbaden, Germany

### 2.1.4 Equipment

Device	Corporation and Location
Neubauer Zählkammer	Optik Labor, Homburg, Germany
Pipettes 10µl, 100µl, 1000µl,	Eppendorf, Hamburg, Germany
FACS Calibur	BD Bioscience, Heidelberg, Germany
Light microscope	Zeiss, Göttingen, Germany
Incubator Heraeus	Thermo, Schwerte, Germany
Sterilbank	Thermo, Schwerte, Germany
Centrifuge	Thermo, Schwerte, Germany
Multi Dispenser	Eppendorf, Hamburg, Germany



## 2 Material and Methods

Ax70 fluorescence microscope	Olympus, Hamburg, Germany
Casyton	Roche, Mannheim, Germany
Casyton tubes	Roche, Mannheim, Germany
HWM D400 IR-device	HWM GmbH, Markdorf, Germany
PipetBoy	Integra Lifesciences, New York, USA
Vortex Genie 2	Scientific Industries, Bohemia NY, USA
Centrifuge 5417R	Eppendorf, Hamburg, Germany
Fridge -20 °C	Liebherr, Biberach, Germany
EL800 Photometer	BioTek Instruments, Winooski VT, USA
gel electrophoresis chamber	Inhouse workshop, Ulm University, Germany
Thermomixer	Eppendorf, Hamburg, Germany
Power Supply 2197	LKB, Bromma, Sweden
Trans-Blot SC	Bio-Rad, Munich, Germany

### 2.1.5 Materials

Material	Corporation and Location
Tissue culture flask 12, 5cm <sup>2</sup>	BD Falcon, Heidelberg, Germany
Tissue culture flask 75cm <sup>2</sup>	Sarstedt, Newton, USA
Tissue culture flask 75cm <sup>2</sup>	Sarstedt, Newton, USA
FACS tubes	Sarstedt, Newton, USA
Tube 15ml	Sarstedt, Newton, USA
Tube 50ml	Sarstedt, Newton, USA
Eppendorf- Reaktionsgefäß	Eppendorf, Hamburg, Germany
CellStar®cell culture 12- well	Greiner, Kremsmünster, Austria
DesoMedian®	Desomed AG, Freiburg, Germany
Desomed Rapid AF	Desomed AG, Freiburg, Germany
Serological Pipette 25ml	Sarstedt, Newton, USA
Serological Pipette 10ml	Sarstedt, Newton, USA
Serological Pipette 5ml	Sarstedt, Newton, USA



## 2 Material and Methods

Serological Pipette 2ml	BD Falcon, Heidelberg, Germany
Pipet tip 1250 µl long	Sarstedt, Nümbrecht, Germany
Pipet tip 200 µl yellow	Sarstedt, Nümbrecht, Germany
Pipet tip 20 µl neutral	Sarstedt, Nümbrecht, Germany
MicroTouch® nitrile gloves	Ansell, Staffordshire, UK
Peha-soft® nitrile	Hartmann, Heidenheim, Germany
CultureSlides	BD Falcon, Heidelberg, Germany
100x20mm Tissue culture dish	Sarstedt, Newton, USA
Cell Scraper 25cm	Sarstedt, Newton, USA

### 2.1.6 Software

Program	Corporation and Location
Microsoft Excel 2010	Microsoft, Washington, USA
Flowing Software 2 V.2.41	University of Turku, Turku, Finland
Gen5 V1.07	BioTek Instruments, Winooski, USA
MATLAB	The MathWorks, Massachusetts, USA
ImageJ V1.47	National Institutes of Health, USA

## 2.2 Methods

### 2.2.1 Cell culture

Cell culture work was accomplished under aseptic conditions by using a clean bench with laminar airflow. Cells were incubated at 37°C and 5% CO<sub>2</sub>. Cell line U87MG was obtained from ATCC and cultured in tissue culture flasks (75cm<sup>2</sup>) containing DMEM supplemented with 10% FCS and 2% penicillin/streptomycin. TIC (G35, G38) specimens were chopped up in ice-cold PBS and centrifugated 5 min at 345g at room temperature. After discharging the liquid, the tumor pallet was trypsinated for 5 minutes under incubation. In addition, tumor cells were filtered through a sieve with 70µm pore size



## 2 Material and Methods

and taken up in TIC cell medium [110]. TIC were cultured in non-tissue culture flasks (75cm<sup>2</sup>) containing DMEM/F12, supplemented with 2% B27, 2% Amphotericin B, 1% penicillin/streptomycin, 20µg/ml EGF and 10µg/ml FGF.

For experimentation, differentiated cells (G38dif and G35dif) were derived from corresponding TIC. Therefore, TIC were differentiated by putting them into tissue culture flasks (75cm<sup>2</sup>) containing DMEM supplemented with 15% FCS, 2% Amphotericin B, 1% penicillin/streptomycin, 1% L-glutamine and 2,5% HEPES Buffer.

### 2.2.2 Detaching adherent cells

Adherent cells were detached with a Trypsin and EDTA solution (0,05% Trypsin 0,02% EDTA) for 5 minutes.

### 2.2.3 Counting Cells

Cell count for seeding was determined microscopically (optical enlargement 10x) with a counting chamber (Neubauer-improved). Cells were counted on four quadrants and the average number was calculated by formula 1:

$$\frac{\text{Number of cells}}{4} = [\text{Cells}] * 10^4 \quad (1)$$

### 2.2.4 Seeding cells

After counting as described, cells were seeded with a density of  $0,5 * 10^4$  cells/qcm. The total number of cells was calculated by equation 2:

$$\text{total amount of cells} = \frac{0,5 * 10^4 [\text{cells}]}{[\text{qcm}]} * \text{growth area} [\text{qcm}] \quad (2)$$

The amount of cells were attenuated in the corresponding amount of medium.



### 2.2.5 $\gamma$ -Irradiation

Cells were irradiated with  $^{137}\text{Cs}$  radiation source HWM D400 (44Tbq, 2Gy/min) at the Zentrum für Biomedizinische Forschung, located at Oberer Eselsberg Ulm.

### 2.2.6 Cell count measure with CASY®

Cells were harvested and attenuated in 10ml CASYton medium. Cell count per milliliter was determined with CASY® cytometrically.

### 2.2.7 Measuring DNA fragmentation via Fluorescence Activated Cell Sorting (FACS)

Cytometry is a rapid method for analysing cells on a single cell basis. For this study we used FACSCalibur from BD Bioscience for measuring DNA fragmentation. Here, cells are examined by the reflection of LASER beams, which get detected by front and side photomultipliers. Therefore cells can be divided by size and granularity or by fluorescence staining. FACS data was analyzed with Flowing Software 2.

### Cell cycle analysis and Cell death measure by Fluorescence labeling with Propidium Iodid (PI) “Nicoletti”

Adherent cells were detached as described in 2.2.2 and centrifugated for 5 minutes at 1800rpm together with their medium. In addition supernatant was discarded. For cytometry, cells were incubated with 0.1 % Trisodium citrat dihydrat, 0.4 % Triton-X 100 and 50 $\mu\text{g}/\text{ml}$  PI for 10 minutes. In this procedure, Triton X perforates the cellular membrane and PI, as a fluorescence dye, intercalates with DNA. As the fluorescence signal correlates with the amount of DNA, cells can be sorted by DNA content. These groups can be assigned to different cell cycle phases, with single DNA content (G1-peak), doubled DNA content (G2/Mitosis-peak), intermediate DNA content (S-peak) or beyond doubled DNA content (Polyploid). Cells with minor DNA content than the G1-peak (subG1 peak)



## 2 Material and Methods

are regarded as dying cells, as DNA fragmentation is a hallmark of apoptosis [72]. Percentage of SubG1 cells was calculated by subG1 cell count divided by total cell number. Specific apoptosis was calculated by formula 3:

$$\text{specific apoptosis} = \frac{\text{SubG1(Probe)} - \text{SubG1(Control)}}{100 - \text{SubG1(Control)}} \quad (3)$$

Percentage of cell cycle phases was calculated by the specific cell number divided by viable cell number. For cell cycle analysis, at least 10000 cells were counted, for specific apoptosis analysis 5000 cells were counted.

### 2.2.8 Immunohistochemical staining of $\gamma$ H2AX

Phosphorylation of Histon H2A is an early step in DNA damage response, especially to DNA double strand breaks [22]. Staining of phosphorylated H2AX (syn. pH2AX or  $\gamma$ H2AX) is the best available standard for detecting double strand breaks [100]. Therefore, cells were counted and seeded on culture slides (0.69cm<sup>2</sup>) as described. Cells were washed twice with PBS before fixation for 10 minutes with 3.7% paraformaldehyde. In addition cells were washed again twice and treated with 0.5% TritonX for 5 minutes for permeabilisation of cellular membrane layers. After another round of PBS-washing, cells were kept for at least one hour in 10% FCS at 4°C in order to block unspecific bindings. The primary antibody mouse anti- $\gamma$ H2AX was attenuated 1:100 in 10% FCS and incubated at 4°C overnight. In addition, cells were washed four times with FCS, five minutes each. The second antibody goat anti-mouse was incubated at 4°C for one hour with an 1:200 attenuation in FCS. Because of its fluorescence labeling, this and all further steps were kept in the dark. Finally, cells were washed another three times in 10% FCS and prepared with mounting medium for microscopical investigation. Microscopical work was done on Olympus AX70 fluorescence microscope, and corresponding software. Cells were counted  $\gamma$ H2AX positive, if more than 9 fluorescence spots were counted. At least 75 cells per probe were counted.



### 2.2.9 Western Blot

Western Blot is a qualitative method for detecting cellular proteins. Cells were seeded at 100x20mm tissue culture dishes and cultured for adherence overnight as described. At time point of measure, medium was discarded and cells were harvested with a cell scraper on ice cold PBS Buffer. All further steps were done on ice. After washing with PBS (5min, 1800rpm, 5 °C) cells were put into 1.5ml tubes and frozen at -20 °C.

For protein extraction, cellular proteins were lysed with lysisbuffer (30 mM TRIS, 150 mM sodium chloride, 1% Triton X und 10% glycerol) and incubated 15 min on ice. After centrifugation at 13000 rpm at 4 °C for 20min the sustained was put into new 1.5ml tubes on ice. In order to get the same amount of protein in every slot we used a photometric determination of protein level. Therefore we performed a standard-protein assay according to the following BSA-Standard: 2000µg/ml, 1500µg/ml, 1000µg/ml, 750µg/ml, 500µg/ml, 250µg/ml, 125µg/ml, 62.5µg/ml. The Pierce BCA Protein Assay Kit was mixed 50:1 Reagent A : Reagent B. Then 1 µl of every probe was mixed up with 200µl Pierce reagent, incubated for 15min at 37 °C, 5%CO<sub>2</sub> and analysed photometrically. The Pierce BCA Protein Kit integrates several steps known as the Biuret Reaction: Peptides with two peptide bindings at least, build up chelat complexes with Cu<sup>2+</sup> and thereby mask the copper. An alcalic solution reduces the copper ions and leads to a drop out of the copper ions in a second step. BCA is added and two BCA molecules and a copper ion build a complex with a photometric peak at 562nm. Therefore we can conclude from the measured photometric intensity to the protein level. Probes were analysed with EL800 Photometer by BioTek Instruments and the corresponding software Gen5. In order to get 40µg protein per slot, the probes were mixed up with water according to the protein concentration and 3µl 6x loading dye (7ml Upper Gel Buffer(12.11g TRIS; 8ml 10% SDS; 200ml H<sub>2</sub>O; HCL for ph=6.8); 4ml Glycerol; 100µl 10%SDS; 0.93g DTT; 10mg Bromphenolblue; 10ml H<sub>2</sub>O).

Proteins were separated by size on 12 % SDS-Polyacrylamide Gel Electrophoresis. Therefore we denaturated the Proteins with a Thermomixer at 95 °C for 5 minutes. 12% SDS-Polyacrylamide gel (4.9ml H<sub>2</sub>O; 6.0ml 30% acrylamide mix; 3.8ml 1.5M TRIS (pH



## *2 Material and Methods*

8.8); 0.15ml 10% SDS; 0.15ml 10% ammonium persulfate; 0.006ml TEMED) and 5% stacking gel (3.4ml H<sub>2</sub>O; 0.83ml 30% acrylamide mix; 0.63ml 1.0M TRIS (pH 8.8); 0.05ml 10% SDS; 0.05ml 10% ammonium persulfate; 0.005ml TEMED) were filled up between two glass plates and loaded with a ladder protein marker (4µl) and 21µl of every probe. The glass plates were plugged up with silicon paste and spacers at the bottom and the edge. The gel was applied on 120V, 400mA in the stacking gel for 30min and on 20V, 400mA in the resolving gel overnight. Negatively loaded proteins go from anode to cathode. As big proteins move slower in the viscose gel, proteins get separated by size.

In the next step proteins are transferred from the gel to a nitrocellulose membrane. The nitrocellulose membrane and six whatman membranes were incubated in blotting buffer (11.6g 125mM TRIS; 5.8g 1.25M Glycin; 7.5ml 0.1% SDS 10%; 400ml Methanol 2l H<sub>2</sub>O). The gel and the nitrocellulose membrane enveloped by three whatman membranes on each side were blotted with Trans-Blot SD device at 20V and 120mA for 70 minutes.

In order to block unspecific binding, the membrane was incubated for 60 minutes in blocking buffer (25g 5% milk powder; 50ml PBS; 500µl 0.1% Tween 20) and washed 10 minutes afterwards in washing buffer (PBS; TRIS 1:1000). To detect the wanted protein, the primary antibody (5% BSA - PBS Solution, 0.1% sodium azide) was incubated at 4°C overnight. At the next day, the membrane was washed three times with washing buffer before the second antibody was incubated for one hour. All incubation was performed with the membrane on a shaking device.

For visualization, we used Pierce Western Blotting Kit to visualize the protein bands. Reagent 1 and 2 were mixed 1:1, put onto the membrane and incubated for one minute. Afterwards we put the membrane into a film cassette in order to protect it from light. In a dark room we put a film onto the membrane and developed it with the corresponding device. Quantitative analysis was performed with ImageJ.



### 2.2.10 Colony Forming Assay

1000 cells were seeded on 12.5cm<sup>2</sup> culture flasks and grown adherently overnight. 10 days after treatment, cells were washed with PBS and fixed in 3.7% paraformaldehyde for 10 minutes and stained with 1:10 Giemsa solution for 10 minutes. After several washes, colonies with more than 10 cells per colony were counted. Cell survival was calculated in % of control and mathematical interpolation was calculated with MATLAB on basis of the linear quadratic model [33] according to equation 4:

$$S(D) = e^{-\alpha D - \beta D^2} \quad (4)$$

### 2.2.11 Data Analysis

Data was analyzed with Microsoft Excel 2010. Statistical significance was calculated by student's t-Test.

In order to evaluate the efficacy of our combination treatments we calculated the expected value ( $E_{1,2}$ = effect of treatment, e.g. % amount of apoptosis) for the combination treatment of two additive, Bliss-independent treatments 1 and 2 [12]. This expected value ( $E_{1,2}$ ) was calculated out of the measured values for treatment 1 ( $M_1$ ) and treatment 2 ( $M_2$ ) according to equation 5. In the following, we compared this calculated value ( $E_{1,2}$ ) with the result of our combination experiments ( $M_{1,2}$ ) and calculated the Bliss-ratio ( $B_{1,2}$ ) between the measured value ( $M_{1,2}$ ) and the calculated value ( $E_{1,2}$ ) of Bliss-independent treatments according to equation 6. For evaluation about the additivity we interpreted this ratio as follows: <0.95: treatments likely to be less than additive or antagonistic; 0.95-1.05: treatments likely to be additive, >1.05: treatments likely to be more than additive or synergistic.

$$E_{1,2} = M_1 + M_2 - (M_1 * M_2) \quad (5)$$

$$B_{1,2} = \frac{M_{1,2}}{E_{1,2}} \quad (6)$$



## 3 Results

### 3.1 Effects of irradiation on glioblastoma cells

#### 3.1.1 Cell Survival Curve for G35dif

The susceptibility to radiotherapy differs highly among different types of cancer [99]. To measure the radiosensitivity of our primary cells G35dif we performed a colony forming assay. Cells were irradiated with 1Gy, 2Gy, 4Gy, 6Gy and 10Gy and colony formation was determined after 10 days (Fig.4).

The resulting dose response curve was calculated according to the linear quadratic model (solid line). Hereby, the Survival Fraction (SF) is a quantity for the long-lasting reproductive integrity of cells after irradiation and shows a dependence to the irradiation dose. For 1Gy to 6Gy the colony formation showed a linear-exponential decrease (illustrated by the dotted line). For doses higher than 6Gy, cell survival decreased non-linearly which can be seen at the SF(10) value. The percentage of viable colonies at 2Gy irradiation (SF(2)-value) is an index for radiosensitivity among cell lines and was determined as 0.69 for G35dif. Consequently these cells can be considered as radioresistant and do not deviate from other glioblastoma cell lines (see Table 1). As seen in Fig.4c+d microscopical examination revealed two different types of colonies which could be distinguished by morphology and size. Type 1 cells showed up with a small longitudinal shape ca. 25-50  $\mu\text{m}$ , a non-definable nucleus and bipolar invadopodia (Fig.4c). In contrast type 2 cells were much larger (150-200  $\mu\text{m}$ ) and showed up with a rounded body, big nucleus and multiple invadopodia (Fig.4d). Interestingly the percentage of type 2 colonies increased with irradiation dose and mainly between 6Gy and 10Gy (Fig.4e).

Taken together, with a SF(2) value of 0.69 G35dif can be regarded as a radio-resistant cell population. A linear exponential decrease was seen in colony count up to 6Gy, while non linear effects became visible after irradiation with 10Gy. In addition cell morphology changed towards giant multinucleated cells after high doses of irradiation.



### 3 Results

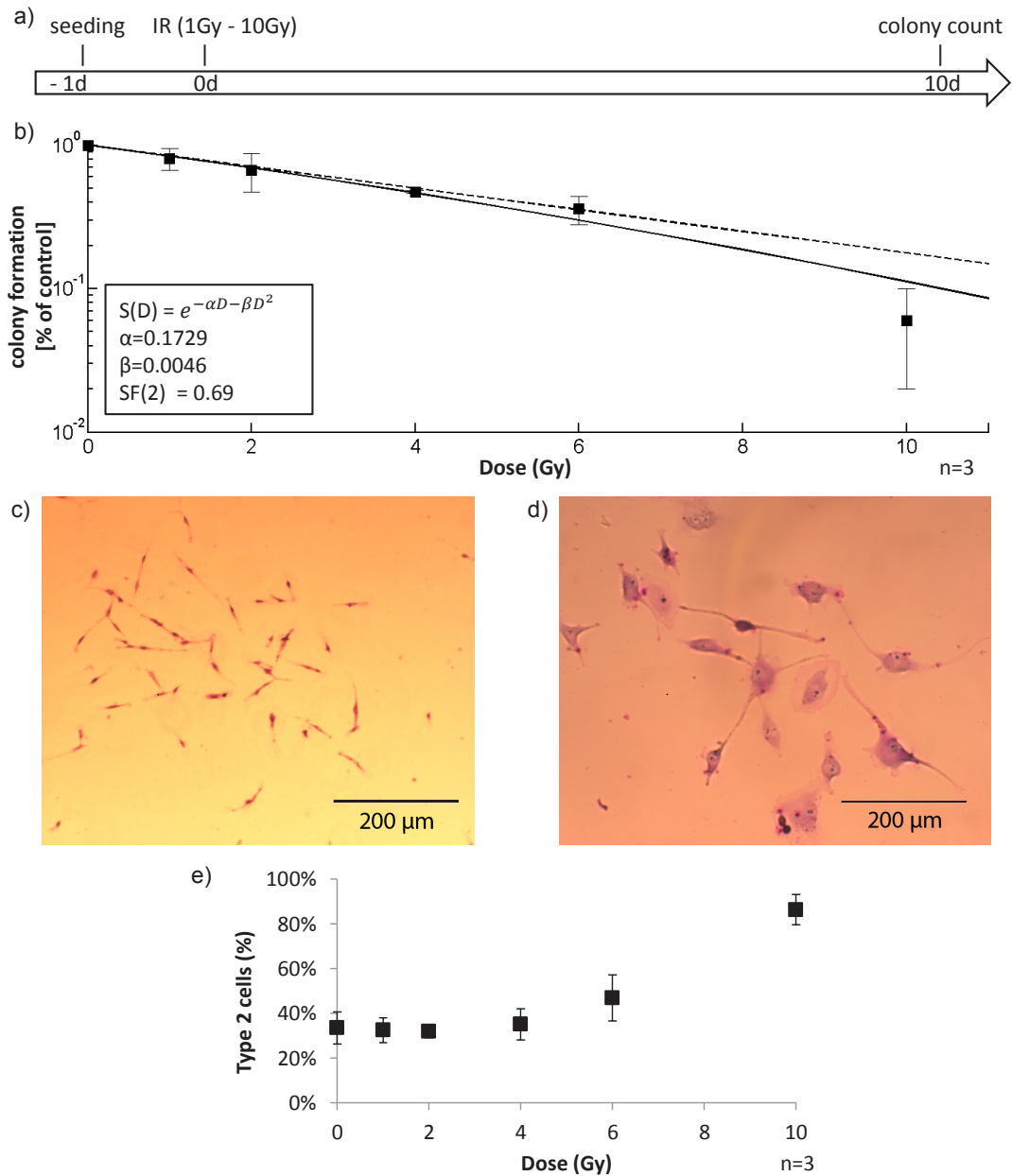


**Figure 4 – Colony forming assay after IR for G35dif** a) Experimental chronology: Cells were irradiated from 1Gy - 10Gy. After 10 days, cells were Giemsa stained and colony numbers were determined. b) Cell survival curve for G35dif: The solid line shows the interpolation according to the linear quadratic model, the dotted line displays the linear part of the equation. The survival value at 2Gy is  $D(2)=0.69$ . c)-d) Microscopical examination of different colony types: The pictures show representative samples of Type I cells (c) and Type II cells (d). e) Percentage of Type II cell colonies among all colonies dependent on irradiation dose; The experiment was performed three times done in triplicates. Error bars indicate standard deviation. Fig. a)-b) have been published in [45] under CC BY 4.0, <https://creativecommons.org/licenses/by/4.0/deed.de>; Fig. c)-e) are republished with permission of Critical reviews in oncogenesis by Begell House Inc Publishers from [37]. Reproduced with permission of Begell House Inc Publishers in the format Thesis/Dissertation via Copyright Clearance Center.



### 3 Results

**Table 1** – SF2 values for different cell lines. G35dif is highly radioresistant similar to other established glioblastoma cell lines compared to tumor cells of other origin or non-neoplastic cells. HNSCC = Head and Neck Squamous Cell Carcinoma

Cell line	Tumor/Cell type	SF2
U87MG [3]	glioblastoma	0.81
A-172 [21]	glioblastoma	0.74
U-138 [21]	glioblastoma	0.72
T98G [95]	glioblastoma	0.70
<b>G35dif</b>	<b>glioblastoma</b>	<b>0.69</b>
HeLa [41]	adenocarcinoma	0.41
SCC61 [3]	HNSCC	0.36
U-622CG [73]	glia (non neoplastic)	0.25
HF19 [29]	Fibroblast (non neoplastic)	0.20

#### 3.1.2 Differences between single dose and fractionated dose radiation for G35dif and G38dif

As described previously, clinical glioblastoma radiation therapy is currently administered in 2Gy fractions given five times a week for a total of 60Gy [98]. The fractionation of 2Gy emerged because of clinical experience about acceptable acute and late side effects in humans [114]. According to this, we designed a protocol for Fractionated Dose Irradiation (FD-IR) in order to work as close to the clinical situation as possible. Though, Single Dose Irradiation (SD-IR) up to 10Gy is frequently used for in vitro settings by many scientists for practical reasons. As part of this work, we examined similarities and differences of SD-IR and FD-IR irradiation schemes.

#### Specific apoptosis, cell count and cell cycle in SD-IR and FD-IR with a total of 10Gy and 5Gy in G35dif glioma cells

First, we applied the weekly radiation scheme from the clinic to our cells in vitro. Cells were seeded 24h before treatment and irradiated 5 times every 24h with 1Gy and 2Gy in the FD-IR groups (Fig.5a). The SD-IR groups were irradiated only once with 10Gy and 5 Gy respectively, together with the first FD-IR dose. 120h, 144h and 168h after



### 3 Results

the first irradiation, cell count, specific apoptosis and cell cycle were determined with a PI-staining and a cytometer.

Fig.5b shows a significant difference in specific apoptosis between FD-IR and SD-IR at all times of measurement for a total of 10Gy. The SD-IR group ranged at 50% specific apoptosis at 120h and 144h and rised up to 64% at 168h. The FD-IR lead to 30% specific apoptosis at 120h and 140h and rised up to 50% at 168h, indicating that the FD-IR provoked significantly less apoptotic cells than SD-IR. In addition, cell count (Fig.5c) was decreased significantly for the SD-IR groups. Here SD-IR lead to a reduction in cell count to around 20% of control at all time points while the cell count for FD-IR was between 27% and 31%. Regarding cell cycle, differences between SD-IR and FD-IR continue to exist. In both groups, irradiated samples showed reduced G1 peaks and elevated S-phase- and G2 peaks along with emerging polyploid cells. At a total of 10Gy (Fig.5d-f), S-phase peaks were significantly higher in the SD-IR groups than in the FD-IR ones, for example in Fig.5d where SD-IR lead to 16% S-phase cells compared to 7% in the FD-IR group. To the contrary, G2 peaks were significantly higher in the FD-IR groups, possibly indicating higher rates for G2 cell cycle arrest by cells undergoing DNA damage repair.

Taken together, 10Gy SD-IR lead to higher rates of cell death and reduced cell count at indicated time points than 5x2Gy FD-IR.

Irradiation with 5Gy revealed similar findings between SD-IR and FD-IR like 10Gy, although differences were expressed to a minor extent. As seen in Fig.5b, SD-IR groups showed higher rates of specific apoptosis (23% after 120h, 16% after 144h and 33% after 168h) compared to the FD-IR groups (15% after 120h, 13% after 144h and 26% after 168h), with significant differences at 168h. Cell count (Fig.5c) sustained this finding. The SD-IR groups showed lower cell count than the FD-IR groups at all times of measurement and differences were significant at 144h and 168h. Cell cycle analysis (Fig.5g-i) showed a G1 reduction in all irradiated samples from about 70% of all viable cells in the control to about 55% in the irradiated samples. These cells (15%) mainly apporportioned to the G2 phase and the polyploid group. In SD-IR groups the S-phase was increased,



### 3 Results

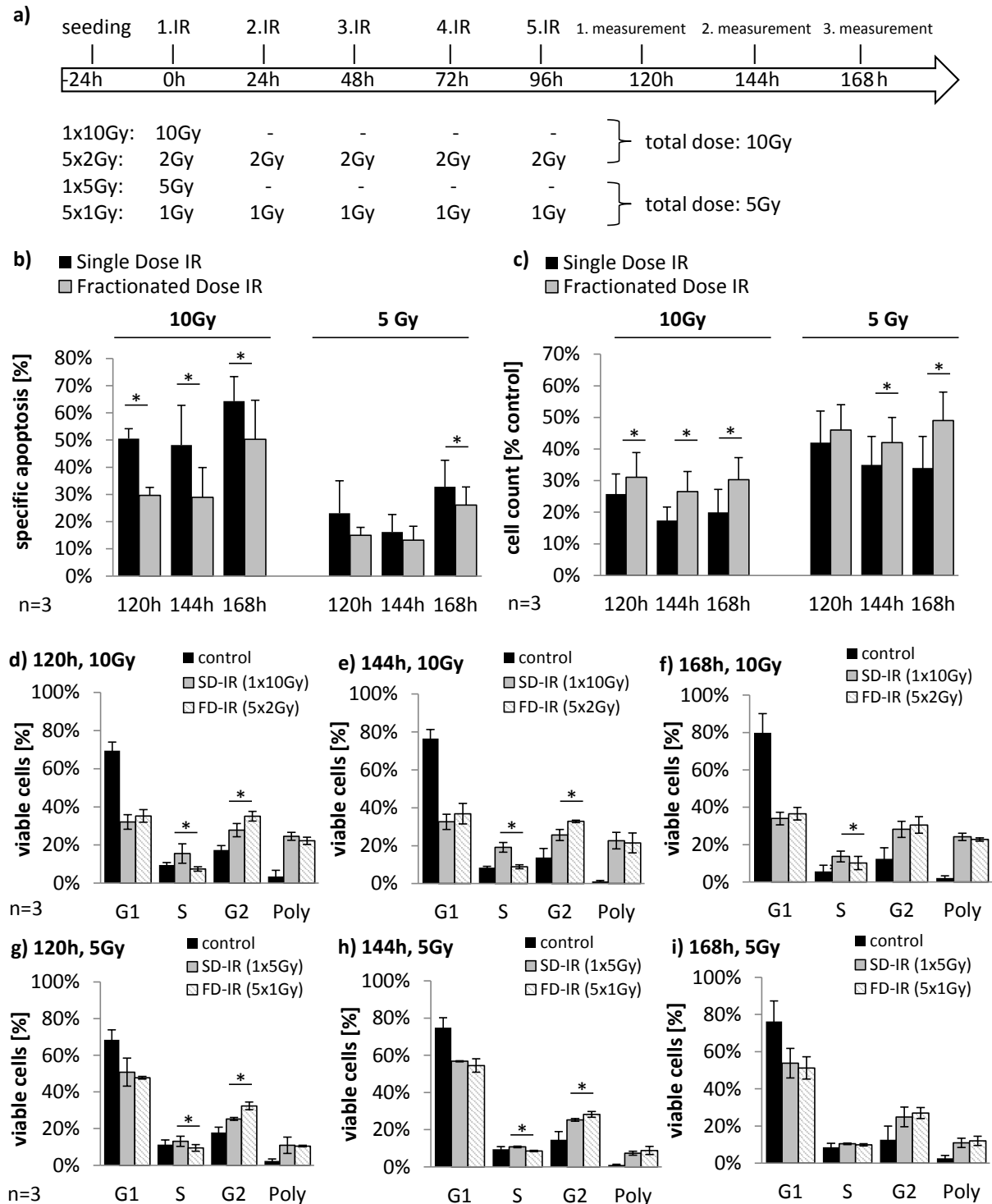


**Figure 5 – Differences between Single Dose Irradiation (SD-IR) and Fractionated Dose Irradiation (FD-IR) with a total of 10Gy and 5Gy for G35dif** a) Experimental chronology: Cells were seeded 24h before the first radiation (1.IR), and re-irradiated or mock treated every 24 hours. Measurements were performed at 120h, 144h and 168h. b) Specific apoptosis was calculated on the basis of DNA-fragmentation, measured by flow cytometric analysis of propidium iodide-stained nuclei. c) Viable cells were measured with CASY cytometer. d)-i) Cell cycle distribution was calculated on the basis of flow cytometric analysis of viable propidium iodide-stained nuclei. The experiment was performed three times done in triplicates. Error bars indicate standard deviation. \* indicates significance  $p < 0.05$ . Data collection in cooperation with S. Stroh. This figure has been published in [45] under CC BY 4.0 <https://creativecommons.org/licenses/by/4.0/deed.de>



### 3 Results

while the G2-phase was reduced towards the FD-IR group. This result was significant for 120h and 144h.

Taken together, SD-IR leads to higher rates of cell death and reduced cell count at indicated time points than FD-IR. In general, SD-IR and FD-IR for a total of 5Gy sustain the findings of the 10Gy groups, although differences are expressed to a minor extent.

#### **Specific apoptosis, cell count and cell cycle in SD-IR and FD-IR with a total of 10Gy and 5Gy in G38dif glioma cells**

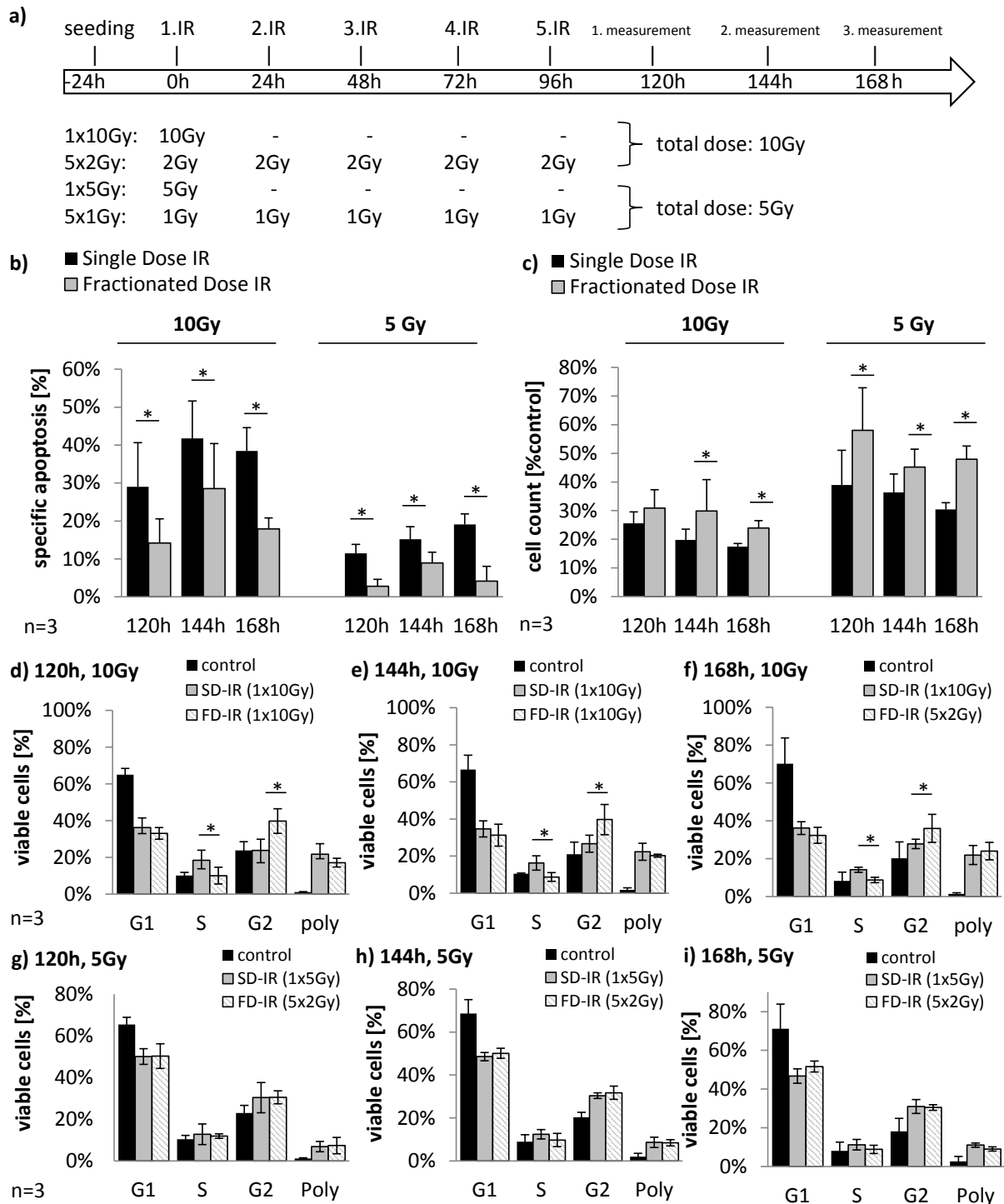
In order to elucidate the impact of this phenomenon, we repeated this experiment with G38dif cells, another primary cell line (Fig.6). Like in the previous experiment, cells were seeded 24h before treatment and irradiated 5 times every 24h with 2Gy/1Gy in the FD-IR group (Fig.6a). In the SD-IR group, cells were irradiated only once with a total dose of 10Gy or 5Gy respectively. 120h, 144h and 168h after the first irradiation, cell count, specific apoptosis and cell cycle were determined with a PI-staining and a cytometer.

Fig.6b shows significant differences in specific apoptosis between FD-IR and SD-IR at all measurements for a total of 5Gy and 10Gy with again SD-IR inducing significant higher apoptosis than FD-IR. Cell count (Fig.6c) was reduced more in SD-IR than in FD-IR. Analysis of cell cycle (Fig.6d-f) showed prominent reduction of G1-peaks for irradiated cells and increased S-phase, G2-phase and emerging polyploid peaks. Comparing the SD-IR with FD-IR samples S-phase was increased for SD-IR, while the G2-phase was reduced towards the FD-IR group. This difference was significant at all three times of measurement for the 10Gy group while differences declined for the 5Gy group (Fig.6g-i).

Taken together, SD-IR lead to higher cellular damage with increased rates of apoptosis and reduced cell count compared to the FD-IR scheme for both primary cell lines. In addition cells in G2 phase were increased and S-phase were reduced in FD-IR groups compared to SD-IR.



### 3 Results



**Figure 6 – Differences between Single Dose Irradiation (SD-IR) and Fractionated Dose Irradiation (FD-IR) with a total of 10Gy and 5Gy for G38dif** a) Experimental chronology: Cells were seeded 24h before the first radiation (1.IR), and re-irradiated or mock treated every 24 hours. Measurements were performed at 120h, 144h and 168h. b) Specific apoptosis was calculated on the basis of DNA-fragmentation measured by flow cytometric analysis of propidium iodide-stained nuclei. c) Viable cells were measured with CASY cytometer. d)-i) Cell cycle distribution was calculated on the basis of flow cytometric analysis of viable propidium iodide-stained nuclei. The experiment was performed three times done in triplicates. Error bars indicate standard deviation. \* indicates significance  $p < 0.05$ . Data collection in cooperation with S. Stroh. This figure has been published in [45] under CC BY 4.0, <https://creativecommons.org/licenses/by/4.0/deed.de>



#### 3.1.3 Irradiation protocol for multitarget therapy with a total of 6Gy for G35dif

As the tendency between SD-IR and FD-IR was similar between 120h, 144h and 168h we chose 120h as the time of measurement in order to minimize unspecific effects. For further experiments we chose 2Gy as the dose for irradiation, because it is the common dose for irradiation in the clinic and it provoked visible effects in our cell culture system. Again, in this thesis we had the aim to stay as close to the clinical situation as possible and therefore irradiated the cells every 24 hours. Next, we chose a total dose of 6Gy and reduced the FD-IR to three fractions (3x2Gy) for further experimentation for the following two reasons: First, as 6Gy was still in the linear scope of the cell survival curve, we assumed differences between SD-IR and FD-IR would decline. Second, while 3x2Gy shortens the irradiation treatment time to 48h, it gives better options towards the combination with chemotherapy, which was planned for future experiments. Therefore we first examined the differences between 1x6Gy SD-IR and 3x2Gy FD-IR in specific apoptosis and cell count. Cells were seeded 24h before the first treatment and irradiated with a single dose of 6Gy or with a fractionated dose of 1x2Gy, 2x2Gy or 3x2Gy every 24h (Fig.7a). Cell count (CASY) and DNA fragmentation with a PI-staining (FACS) was measured 120h after the first treatment and specific apoptosis was calculated.

A single dose of 2Gy irradiation lead to 4% specific apoptosis after 120h (Fig.7b). In FD-IR, there was a linear rise with about 4% on every 2Gy additional irradiation. Consequently 2x2Gy showed 7% and 3x2Gy about 11% specific apoptosis. 6Gy SD-IR is very similar to this with 12% specific apoptosis. Cell count (Fig.7c) was reduced about 15%-20% on every 2Gy irradiation treatment. FD-IR 3x2Gy reduced cell count down to 47% while SD-IR 6Gy was about 57% of control. Cell cycle response showed reduced G1 phase with increased G2 and polyploid peaks according to rising doses (Fig.7d).

To sum it up, 6Gy seemed to be a suitable dose for combination therapy with about 12% specific apoptosis and a cell count of 50% of control. Differences between FD-IR (3x2Gy) and SD-IR (6Gy) considering apoptosis and cell count revealed no significance. Consequently, we took the 3x2Gy/1x6Gy scheme for further investigation of molecular differences.



### 3 Results

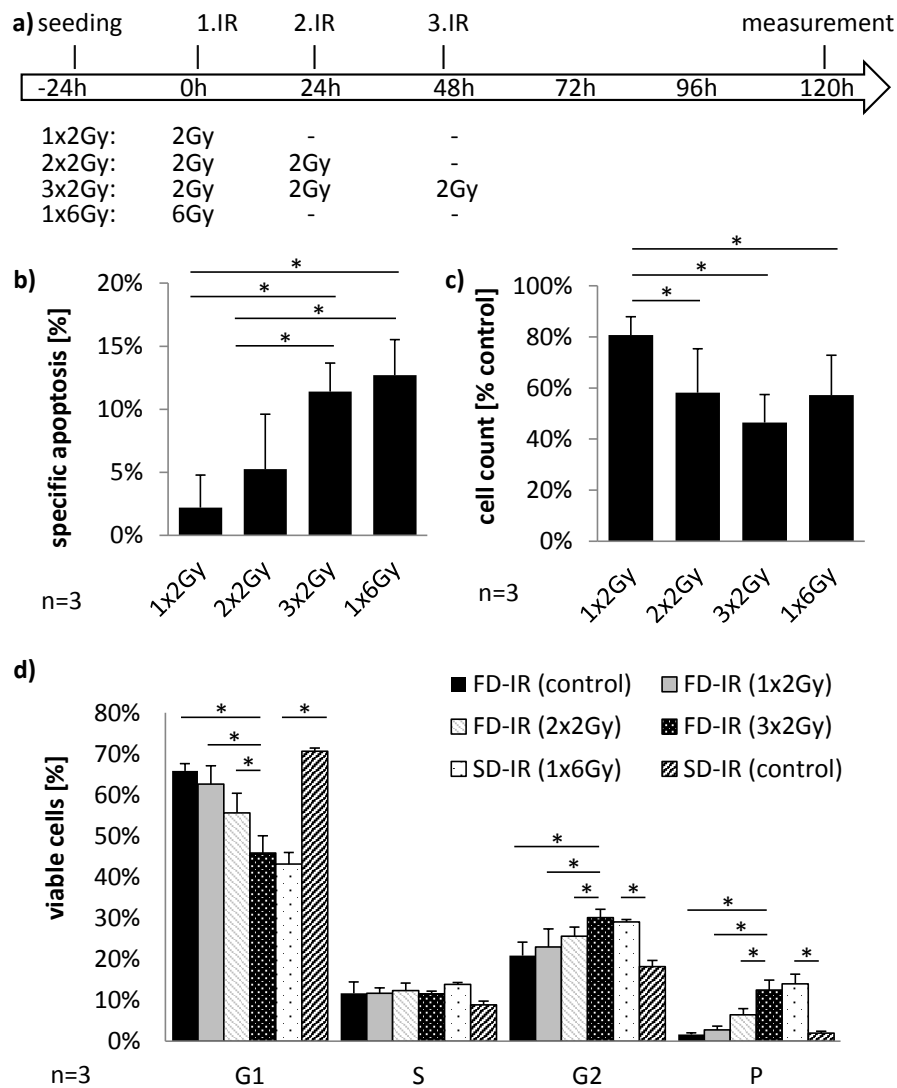


**Figure 7 – Effect of 6Gy SD-IR (1x6Gy) versus 3x2Gy FD-IR for G35dif** a) Experimental chronology: Cells were seeded 24h before the first irradiation (1.IR), and re-irradiated after 24h (2.IR) and 48h (3.IR) depending on group. DNA content was measured with a PI-staining on FACS and cell count was determined with CASY cytometer after 120h. b) Specific apoptosis was calculated from Sub-G1 cell count. c) Cell count in % of control was measured with CASY. d) Cell cycle analysis was performed after 120h by measuring 5000 cells. The experiment was performed three times done in triplicates. Error bars indicate standard deviation. \* indicates significance  $p < 0.05$ . This figure has been published in [45] under CC BY 4.0, <https://creativecommons.org/licenses/by/4.0/deed.de>



### 3 Results

#### 3.1.4 DNA Damage Response after irradiation for a total of 6Gy for G35dif

To monitor cell damage more deeply, we examined molecular difference between SD-IR and FD-IR. As FD-IR induces cell damage repetitively, we first examined the DNA Damage Response (DDR).

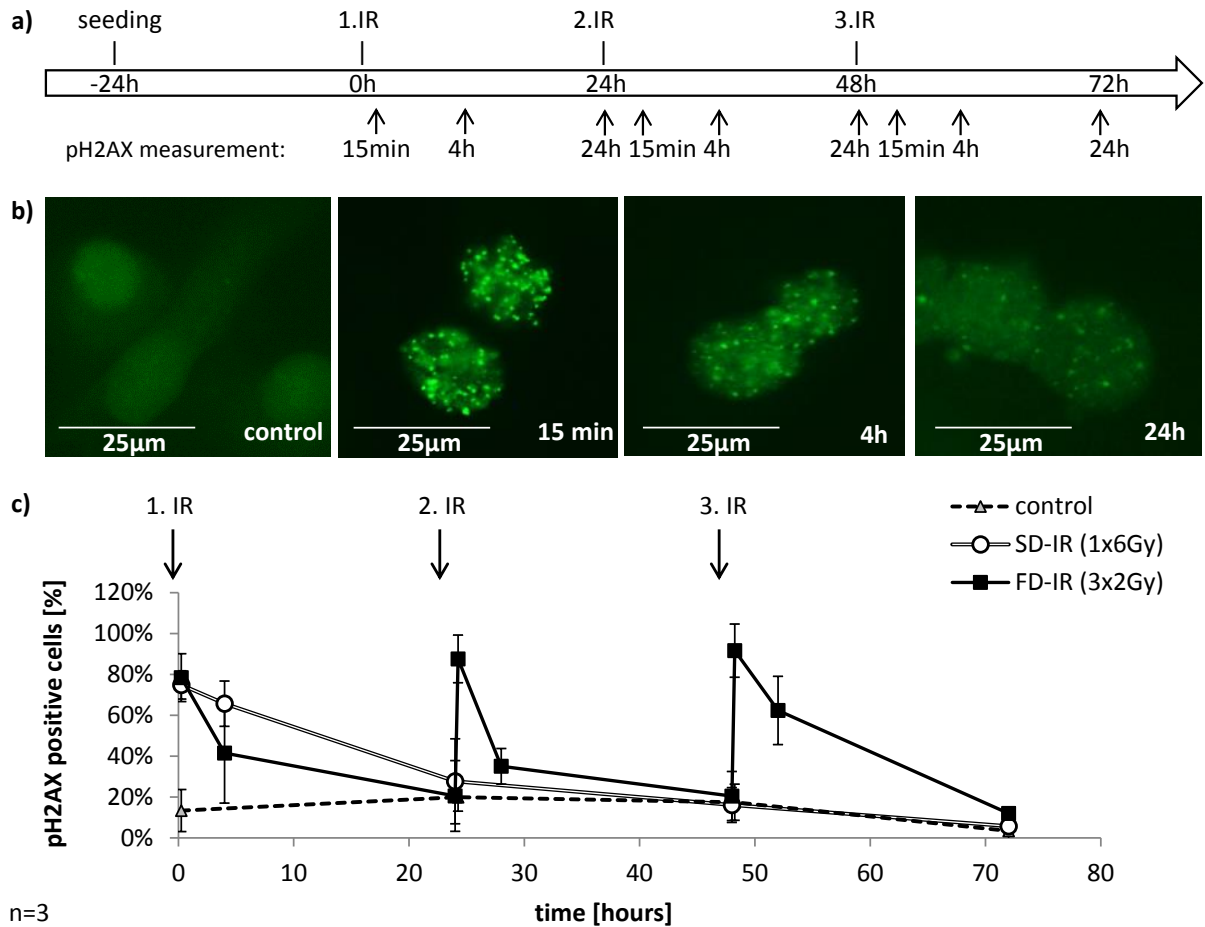


**Figure 8 – DNA Damage Response after IR, via pH2AX staining in G35dif** a) Cells were seeded 24h before the first irradiation and re-irradiated (FD-IR) or mock treated (SD-IR) every 24h. Irradiation was delivered either once (SD-IR 1x6Gy) or in fractions (FD-IR 3x2Gy). Cells were fixed in formaldehyde and immunohistochemically stained with pH2AX as a surrogate marker for DNA damage response and examined with a fluorescence microscope. Cells with more than 10 foci per nucleus were counted positive. b) Representative samples of pH2AX stained cells 15min, 4h and 24h after 2Gy single dose irradiation. c) Percentage amount of pH2AX positive cells were counted 15min, 4h and 24h after each fraction. 1x6Gy SD-IR was examined 15min, 4h, 24h, 48h and 72h after IR. The experiment was performed three times. This figure has been published in [45] under CC BY 4.0, <https://creativecommons.org/licenses/by/4.0/deed.de>



### 3 Results

For this we used a staining of phosphorylated Histon A2 as a very initial marker for DNA damage repair. Cells were seeded 24h before treatment and irradiated either with a 6Gy single dose or with fractions of 2Gy every 24 hours (Fig.8a). Fig.8b shows representative examples of  $\gamma$ H2AX stained cells on various time points after irradiation. In SD-IR and FD-IR, we monitored H2AX phosphorylation over 72h (Fig.8c). Cells were stained 15min, 4h and 24h after each treatment. In the FD-IR group, cells got into an repetitive status of repair directly after each treatment. After 4 hours cells recovered and  $\gamma$ H2AX positive cells declined. To the opposite, 6Gy SD-IR lead to H2AX phosphorylation only once, directly after treatment. While cells stayed positive to 66% after 4 hours, they reach a basal level at 24 hours.

Taken together, cells get  $\gamma$ H2AX positive directly after minutes. FD-IR leads to repetitive activation of DDR after each fraction, while SD-IR gets only activated once after treatment.

#### 3.1.5 Protein status and cell cycle after irradiation in G35dif

Cell cycle response after irradiation may be either induced by p53 mediated p21 induction, or, more rapidly, by Cyclin D1 degradation [1]. As we could show differences between SD-IR and FD-IR, we examined if this finding was reflected on protein level. Therefore we chose KU70, KU80 as direct DNA repair enzymes and p53, p21 and cyclinD1 proteins as cell cycle regulators for Western Blot analysis. Cells were seeded 24 hours before treatment with 3x2Gy FD-IR and 1x6Gy SD-IR. Cells were collected 3 hours and 120 hours after the first fraction of IR.



### 3 Results

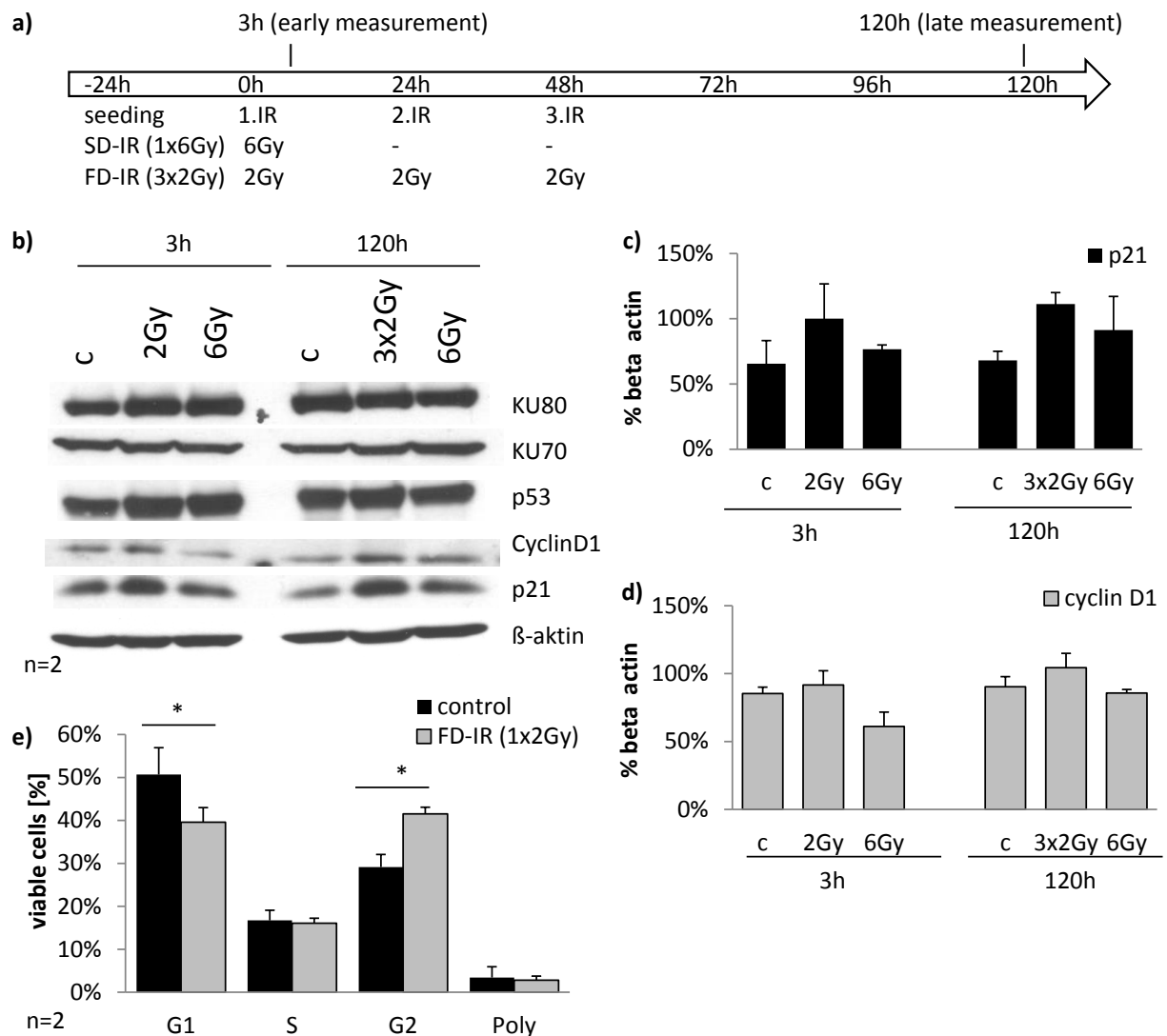


**Figure 9 – Protein expression level of cell cycle regulators at 3h and 120h after 1x6Gy SD-IR and 3x2Gy FD-IR (a-d) together with cell cycle analysis at 6h after 2Gy IR (e) for G35dif** a) Experimental chronology: Cells were seeded 24h before treatment and treated with 3x2Gy and 6Gy, respectively. 3h (2Gy and 6Gy) and 120h (3x2Gy and 6Gy) after treatment cells were harvested, protein extracted and a Western Blot analysis was performed. b) Western Blot analysis was performed for KU70, KU80, p53, p21 and CyclinD1 proteins.  $\beta$ -actin served as loading control. c)+d) p21 and CyclinD1 protein level were quantified according to  $\beta$ -actin control. c=control. Data collection in cooperation with S. Strohm. The experiment was performed twice. e) Cell cycle distribution 6 hours after treatment with 2Gy and 6Gy was calculated on the basis of cytometric analysis of propidium-iodide stained nuclei. The experiment was performed two times done in triplicates. Error bars indicate standard deviation. \* indicates significance  $p < 0.05$ .

Western Blot analysis (Fig.9b) showed the same amount of protein for KU70, KU80 and p53 in the control samples as well as in the irradiated ones. Interestingly, there was an increased amount of p21 protein in the FD-IR group 3 hours and 120 hours after the



### 3 Results

first radiation (Fig.9c). At 120h, p21 is slightly elevated for 6Gy SD-IR, with the effect being less pronounced than for FD-IR. Further, Cyclin D1 levels 3 hours after treatment (Fig.9d) were decreased for 6Gy. At 120h after the first treatment, no differences between the groups become visible for Cyclin D1. As these findings were very small and not significant, they could though indicate a modulation of cell cycle distribution as those proteins have a direct impact on it. Therefore, we examined cell cycle distribution 6h after radiation with 2Gy (Fig.9e). Therefore, cells were seeded 24 hours prior to treatment and irradiated with 2Gy. Cell cycle was determined after 6 hours with a PI-staining on a cytometer. Indeed, the cell cycle is affected by radiotherapy with a significantly reduced amount of G1 cells and an increased amount of cells in G2-phase. There were no differences regarding S-phase and polyploid cells.

Taken together, differences in cell cycle distribution and regulation between SD-IR and FD-IR could be detected.

**In conclusion** we hypothesized that SD-IR initiates the repair cascade only once while FD-IR cells have to go through it on every IR application. As FD-IR is closer to the clinical situation in which the patients get irradiated every 24 hours with a 2Gy fraction, it is the scheme suitable for intracellular pathway examination and the appropriate scheme for further experimentation. **Accordingly we chose the FD-IR model for further experimental procedures.**



## **3.2 Multitarget chemotherapy in combination with ionizing radiation on glioblastoma cells**

Combination therapy of non-selective chemotherapy and selective targeted therapy is a promising approach in glioblastoma treatment [75]. In this study we applied RIST-therapy (Rapamycin, Irinotecan, Sunitinib, Temozolomide) and alternative RIST (aRIST)-therapy (GDC-0941, Irinotecan, Sunitinib, Temozolomide) to our newly established radiation protocol.

### **3.2.1 Effects of multitarget therapy for G35dif and U87MG**

First, we evaluated the effect of RIST/aRIST-therapy on G35dif cells and U87MG cells. Cells were seeded 24 hours before treatment and stimulated with indicated doses (Fig.10a). For both cell lines, the combination of the selective inhibitors Rapamycin/Sunitinib (R/S) and GDC-0941/Sunitinib (GDC/S) did not induce apoptosis (Fig.10b). In contrast, the unspecific chemotherapeutics SN-38 (the active metabolite of the irinotecan prodrug) and temozolomide showed high rates of specific apoptosis in both cell lines with a higher impact on G35dif compared to U87MG. Combination therapy (I/T) had an additive effect for U87 and G35dif. Quadruple therapy (RIST, aRIST) had no additional effect for U87MG, whereas in G35dif cells, a combination of all four substances significantly enhanced apoptosis.

Regarding cell count, small molecule inhibitors and non-selective chemotherapy were highly effective and reduced proliferation significantly. R/S reduced cell count to 46% for U87 and to 28% for G35dif. GDC/S reduced cell count to 65% for U87 and to 52% for G35dif. Combination therapies (IT, RIST and aRIST) were similar effective for U87MG, while RIST and aRIST were slightly more effective than SN-38/Temozolomide (I/T) for G35dif. With better effects on G35dif we used this cell line for further experiments.



### 3 Results

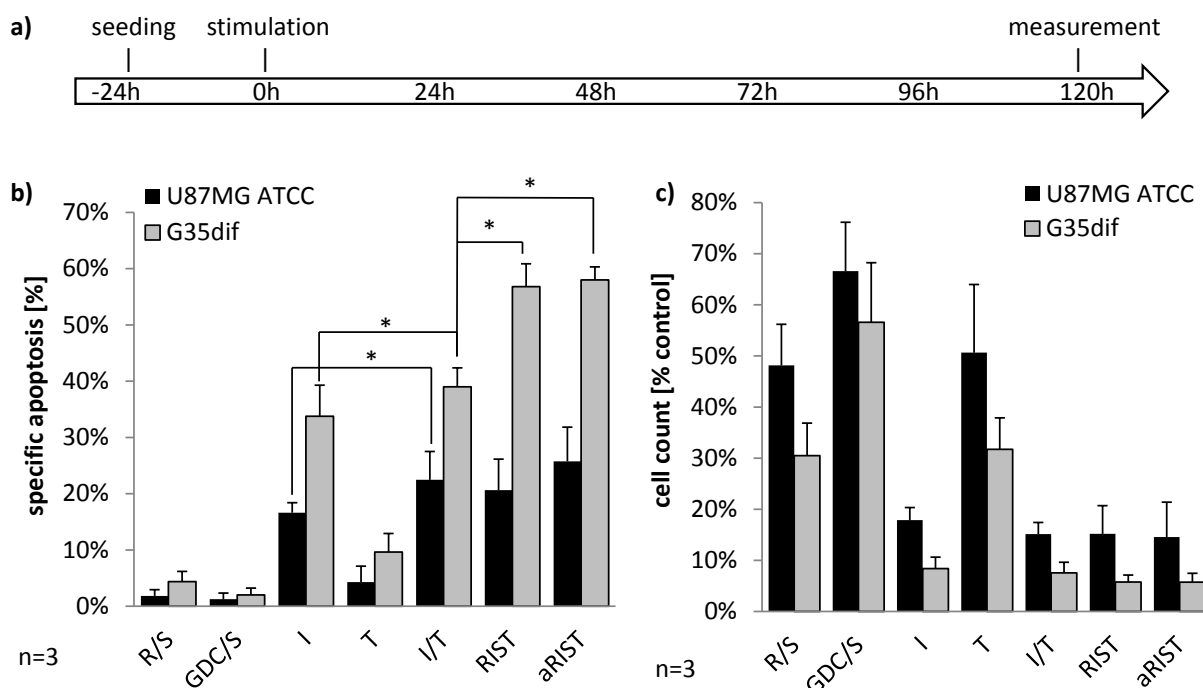


**Figure 10 – The effects of small molecule inhibitors and chemotherapeutic on U87MG and G35dif glioma cells** a) Cells were seeded 24 hours prior to treatment and stimulated with 10nM rapamycin; 0.6μM GDC-0941; 10nM SN-38 (active metabolite of the irinotecan prodrug); 100nM sunitinib and 10μM temozolomide, according to different groups: Rapamycin and sunitinib (R/S); GDC-0941 and sunitinib (GDC/S); SN-38 (I); temozolomide (T); SN-38 and temozolomide (I/T); rapamycin, SN-38, sunitinib, temozolomide (RIST); GDC-0941, SN-38, sunitinib, temozolomide (aRIST). Cells were harvested 120 hours after stimulation. b) Specific apoptosis was calculated on the basis of flow cytometric analysis of propidium iodide-stained nuclei. c) Viable cells were measured with CASY cytometer and cell count was calculated in percentage of control. The experiment was performed three times done in triplicates. Error bars indicate standard deviation. \* indicates significance  $p < 0.05$ . To simplify the diagram, significance is only indicated between I and I/T, and I/T to RIST and aRIST respectively.

#### 3.2.2 Multitarget therapy in combination with ionizing radiation for G35dif

Next, we combined multitarget therapy with ionizing radiation. Cells were seeded 24 hours prior to stimulation (Fig.11a). Chemotherapy was applied directly before the first irradiation cycle in different combinations as described previously. Radiotherapy was applied as FD-IR with 2Gy irradiation every 24 hours for a total of 6Gy.



### 3 Results

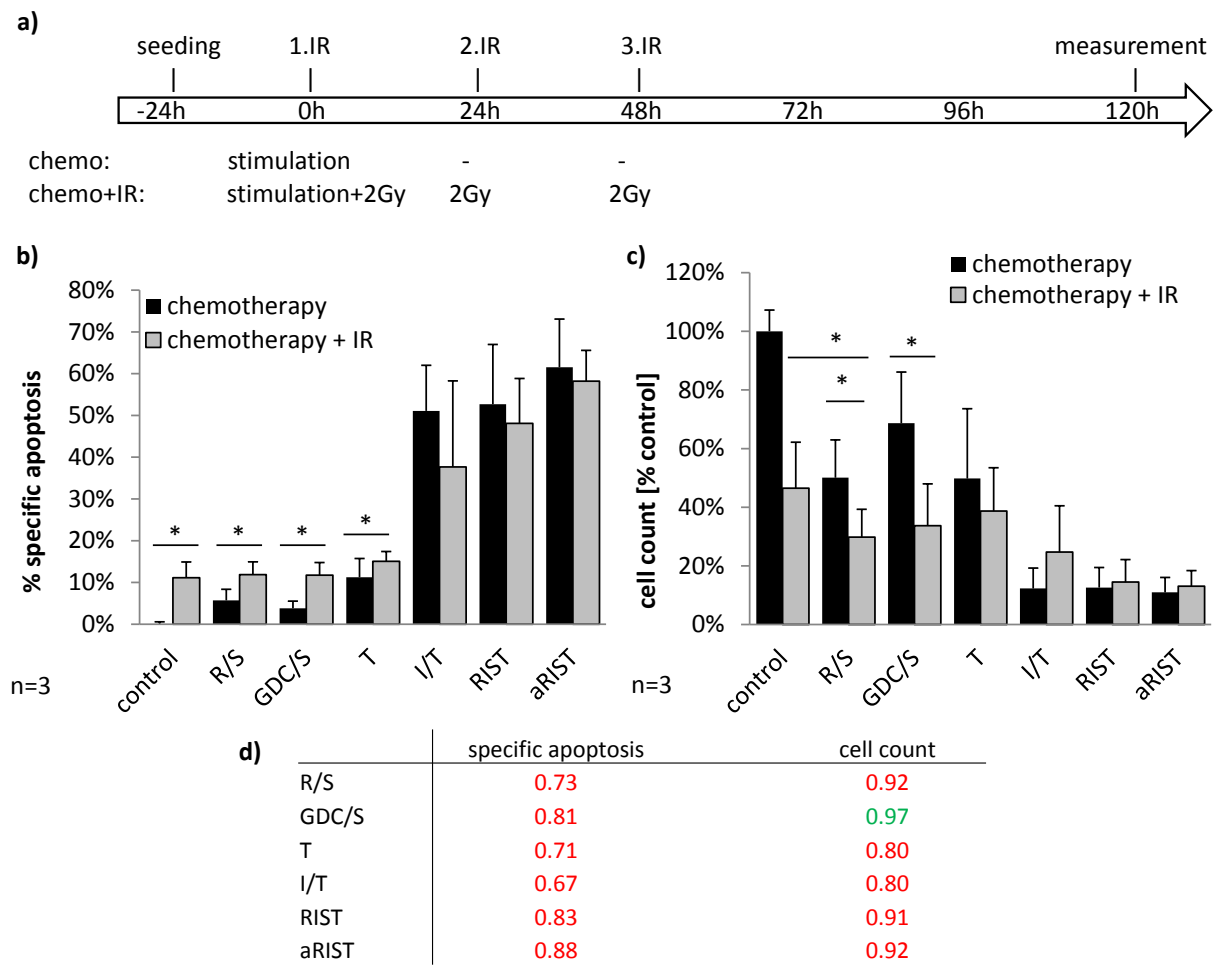


**Figure 11 – Multitarget therapy in combination with ionizing radiation for G35dif** a) Experimental chronology: Cells were seeded 24 hours prior to treatment and co-stimulated with chemotherapy together with the first irradiation dose (2Gy). Chemotherapeutic stimulation with 10nM rapamycin; 0.6μM GDC-0941; 10nM SN-38 (active metabolite of the irinotecan prodrug); 100 nM sunitinib; and 10μM temozolomide according to different groups: Rapamycin and sunitinib (R/S); GDC-0941 and sunitinib (GDC/S); SN-38 and temozolomide (I/T); temozolomide (T); rapamycin, SN-38, sunitinib, temozolomide (RIST); GDC-0941, SN-38, sunitinib, temozolomide (aRIST). Cells were re-irradiated after 24h and 48h, with 2Gy for a total of 6 Gy. Cells were harvested 120 hours after the first stimulation. b) Specific apoptosis was calculated on the basis of flow cytometric analysis of propidium iodide-stained nuclei. c) Viable cells were measured with CASY cytometer and cell count was calculated in percentage of control. d) The Bliss-Ratio between measured and expected values for bliss independent treatments was calculated between irradiated and non-irradiated groups and interpreted for the following: <0.95: treatments likely to be less than additive or antagonistic (red), 0.95-1.05: treatments likely to be additive (green), >1.05 treatments likely to be more than additive or synergistic. The experiment was performed three times done in triplicates. Error bars indicate standard deviation. \* indicates significance p<0.05.



### 3 Results

Cells were harvested after 120h and DNA count was determined by FACS analysis of the DNA fragmentation of propidium iodide-stained nuclei. Cell count was determined cytometrically. Fig.11b shows specific apoptosis for the combination of multitarget therapy in combination with ionizing radiation (chemotherapy + IR) and chemotherapy alone (chemotherapy). 3x2Gy FD-IR without additional chemotherapy induced about 11% specific apoptosis. R/S and GDC/S also ranged at that level with 12% specific apoptosis in the irradiated group compared to 6% (R/S) and 4% (GDC/S) for chemotherapy alone. Consequently radiation had no additional effect regarding specific apoptosis for those groups, which was confirmed by Bliss Analysis (Fig.11d). For I/T, RIST and aRIST, specific apoptosis was even slightly reduced after 120h (Fig.11b).

Though regarding cell count, combination therapy showed an additional effect for R/S+IR (Fig.11c). Nevertheless, the compound effect of radio-chemotherapy is less than the expected calculated additive effect of Bliss-independent treatments as the Bliss-ratio is less than 1 for all groups (Fig.11d). Especially quadruple therapy (RIST, aRIST) and I/T showed lower cell count for chemotherapy alone compared to combination therapy.

To sum up, radiation- and chemotherapy did not profit from combination regarding specific apoptosis and cell count in this experiment.

#### **3.2.3 Intracellular onset of small molecule inhibitors rapamycin, GDC-0941 and sunitinib for G35dif**

In order to get a better understanding of the background to this finding, we focused on the time between chemotherapeutic stimulation and IR application. Therefore we performed a western blot analysis to examine the time of onset of the specific inhibitors R/S and GDC/S. G35dif cells were seeded 24 hours before treatment and stimulated with rapamycin and sunitinib (R/S) or GDC-0941 and sunitinib (GDC/S) respectively. 5min, 15min, 1h, 4h and 24 hours after stimulation cells were harvested and the expression levels and phosphorylation status of AKT (target molecule of GDC-0941) and S6 ribosomal protein (target molecule of rapamycin) were analyzed by western blotting.



### 3 Results

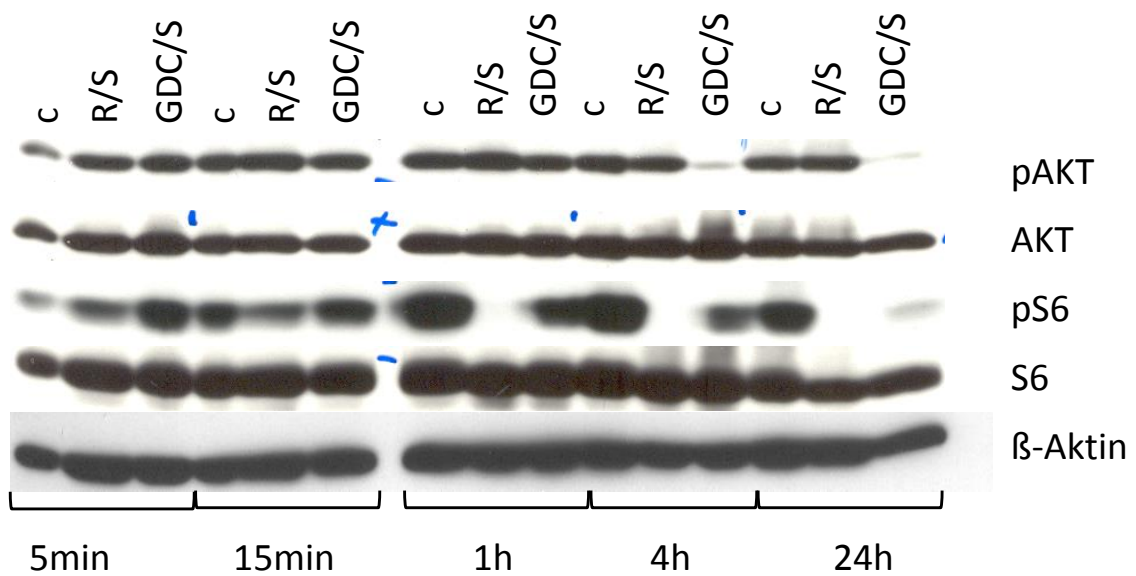


**Figure 12 – Timepoint of onset for small molecules inhibitors rapamycin, GDC-0941 and sunitinib for G35dif** Cells were seeded 24 hours before treatment and stimulated with 10nM rapamycin, and 100 nM sunitinib (R/S) or 0.6μM GDC-0941 and 100 nM sunitinib (GDC/S) respectively. 5min, 15min, 1h, 4h and 24 hours after stimulation cells were harvested and analyzed for pAKT, AKT, S6 and pS6 expression via western blot analysis. β-actin served as loading control. The experiment was performed twice.

Western blot analysis (Fig.12) revealed that after 15 minutes, R/S led to a slight reduction of pS6 level, with a more pronounced effect after 1h. GDC/S led to a reduction of pAKT level after 4 hours. Taken together, R/S combination showed an effect on the target molecule after 1 hour. GDC/S combination lead to reduced pAKT levels and consequent down-regulation of pS6 level after 4 hours post stimulation.



## 4 Discussion

Although glioblastoma patients receive a multidisciplinary treatment, their clinical outcome is still very poor, indicating the need for new therapeutic approaches [111]. Radiotherapy is one of the oldest proven treatments in cancer therapy and still plays an important role in today's treatment [74]. In order to include this established method into new treatment regimen, it is important to know about its cellular and molecular effects in relation to timing and other multitarget therapy drugs. While dose limitation in clinical practice is especially an important feature to consider, this study concentrates on an aspect of equal importance by examining the molecular effects of radiation on primary glioblastoma cells and establishing a radiation protocol on the basis of clinical relevant doses. In the second part we applied this protocol as part of a multitarget therapy regimen.

### 4.1 Effects of irradiation on glioblastoma cells

#### 4.1.1 G35dif in the context of other glioblastoma cell lines

In the present work, G35dif primary glioblastoma cells were examined in respect of ionizing radiation for the first time. With a clonogenic assay, we determined the radiobiological parameter SF2 in Fig.4 as 0.69. The "survival fraction (SF)" indicates the percentage of colonies, and therefore presumably viable seeding cells, after 2Gy irradiation compared to the control group and is a suitable parameter to compare radiation sensitivity between different human tumor cell lines. As summarized in Table 1, glioblastoma cell lines U87MG, A-172, U-138 and T98G have SF2 values between 0.7 to 0.81 [3][21][95], and the SF2 value of G35dif seems to be comparable to those. Notably SF2 values vary to some extent in literature, as the U87 SF2 level ranges from 0.64-0.97 [99] [113], which might be an example for changes in cell lines in different laboratories. Furthermore, G35dif can be considered as radioresistant, as cancer cells from other tissues, like



Adenocarcinoma HeLa cells and Head and Neck Squamous Cell Carcinoma (HNSCC) SCC61 cells, or non-neoplastic cells, like glia cells and fibroblasts, have much lower SF2 values and are consequently more susceptible to radiotherapy [41] [3] [73] [29].

### 4.1.2 Molecular events after ionizing radiation on G35dif

To work up the mechanism of irradiation more deeply and to integrate ionizing radiation (IR) into a multitarget therapy scheme, it is important to investigate the molecular events. With the experiments of this work, it is now possible to show some of the key steps in cellular response after ionizing radiation for G35dif.

#### Initial damage response through H2AX phosphorylation

The first finding is the rapid reaction to cellular damage. Cells initiate damage response directly after irradiation, as pH2AX foci appear directly after minutes (see Fig.8). This is one of the first steps in damage response followed by the recruitment and repair by appropriate proteins. This rapid response confirms the work of Short et al., who showed similar kinetics for U87MG, T98G and A7 glioma cell lines [95].

#### DNA Repair and p53

Proceeding non-homologous end joining (NHEJ) repair, Ku70, Ku80 and DNAPKcs locate at the DNA breaking site, as described in detail in the introduction. Ku70 is widely expressed physiologically in human tissues and also in neuronal glia [19], which might explain the expression in our control groups (Fig.9). Furthermore, as there is strong evidence that Ku70/Ku80 is an obligate heterodimer [28], expression of Ku80 in our control groups might be explained in this way.

Moreover, p53 stabilization and accumulation is a key step in DNA damage response, as described in the introduction. Therefore, the high expression of p53 protein in our control groups is remarkable, as these cells did not acquire DNA damage and p53 levels are normally low in undamaged cells. Therefore we might speculate about a mutant and not



#### 4 Discussion

or aberrant working p53 in G35dif cells, which is a common finding in tumor cells [106] [16]. Of course a control in the blot with known p53 positive and negative cells would be helpful. For further experiments, p53 expression in a healthy astrocyte as a control would be interesting. Furthermore, a DNA sequencing of the p53 gene and a p53 function test [31] could prove p53 gene mutation. In case of a mutant p53, cells might lose control over repair, cell cycle arrest and induction of apoptosis, which enhances radioresistance [67].

#### **Cell death**

Generally, apoptosis as an interphase death may be regarded as a major form of cell death after therapy [14]. For our experiments, we postulate that a post-mitotic form of cell death might be happening especially in the single high dose (>5Gy) irradiated samples because of the following reasons:

Classical Apoptosis is described as an active quick event, with a duration between 4h and 72h, depending on cell type [38]. We might speculate that our cells proceed to cell death long after the initial damaging event, as the percentage of subG1 cells rises with time between 120h and 168h in the 5Gy and 10Gy SD-IR samples (Fig.5b). In addition, Alphonse et al. showed the same result in U87MG glioma cells, as SubG1 peaks emerged not before 72h post 10Gy SD irradiation [3]. This delay hints rather to a form of late apoptosis than to a quick active one. In addition, at our time point of measure (120h) the amount of cells with elevated, polyploid DNA content is increased (Fig.5d-e).

These cells most likely occur during endoreplication without execution of cell division and are described as multinucleated giant cells [102]. In fact, macroscopically enlarged and multinucleated cells also appear in our colony forming assays (Fig.4c-d). Interestingly, these cells increase depending on irradiation dose (Fig.4e). At 10Gy, almost all surviving colonies showed multinucleated cell type for a majority of cells. Here, a staining like Phalloidin/Dapi would make sense in order to prove cellular multinucleation. In this context, Firat et al. could show similar phenomenons with rising numbers of multinucleated cells by time (up to day 7) and irradiation dose (up to 10Gy) in primary p53 deficient glioblastoma cells [30]. Taken together, these hints fit in the picture of a "cell death pre-



## 4 Discussion

ceded by multinucleation" [56], or so called "Mitotic catastrophe". In literature, Mitotic catastrophe has been described as "the major pathway of tumor cell death activated after treatment with ionizing radiation" [102] and as "a process leading to apoptosis" rather than an independent way of cell death. It is characterized as abnormal mitosis after cellular stress (like IR) [83] which might be due to abrogate checkpoint arrest leading to premature entry into mitosis in the presence of unrepaired DNA damage. Depending on multiple parameters, cells can either undergo apoptosis, necrosis or endoreplication to polyploid giant cells [102].

For further research, a kinetics between 0h and 120h with a Annexin/PI/Hoechst-staining on FACS analysis would be very interesting: While Annexin/PI determines the beginning of early apoptosis (Annexin pos./ PI neg.) the Hoechst-DNA co-staining could directly gate the cell cycle fraction of which the dying cells originate. With this experiment, it would not only be possible to see whether cells die out of polyploidy, but also whether the induction of apoptosis begins immediately or later on.

### 4.1.3 Differences in single and fractionated dose irradiation protocol

In the clinic, fractionated radiotherapy with 1.8-2 Gy per fraction has become widespread in glioblastoma treatment during decades of clinical experience and radiobiological research [11]. Nevertheless, SD-IR with high doses of 5Gy, 10Gy or even above is still common practice for in vitro studies (for example [60] [94] [58] [104] [6] [57] [69] [90] [52] [107] [46]). Unfortunately, the comparability between high SD-IR and repetitive low FD-IR is poorly understood. In this work we focused on this issue and present evidence that SD-IR might not be a good surrogate for FD-IR.

### Clonogenic survival, specific apoptosis and cell count

The first difference between high and low IR doses are shown in the clonogenic survival assay (Fig.4). Here, the 10Gy value deviates from the linear-exponential interpolation. The over-exponential decrease of colonies for high doses is a well-known effect and has



#### 4 Discussion

been explained by multiple chromosomal breaks enhancing the chance of mismatched repair [40]. Consequently, it is very likely to achieve additional effects at high dose irradiation above 6Gy for our cells, as 6Gy is the last value on the linear scope of the curve. In this context, differences in specific apoptosis and cell count between SD-IR and FD-IR for a total of 10Gy (Fig.5 and Fig.6) are consistent. Higher rates of specific apoptosis and lower cell count for single dose irradiated cells sustain this theory of increased cell damage at higher doses.

##### **Early differences in DNA Damage Response (DDR)**

On a molecular level, differences between SD-IR and FD-IR become obvious with regard to DDR. While SD-IR cells activate their DDR only once, FD-IR cells are kept in repetitive activation of damage repair (Fig.8). In addition,  $\gamma$ H2AX foci decline after a 2Gy fraction within approximately 4 hours, which is also reported by Zhao et al. [115]. For SD-IR however, H2AX phosphorylation seemed prolonged, which could be explained by enduring repair after higher damage.

On protein level, this finding is confirmed. Although differences are here very subtle and western blot quantification is not a sensitive method, two findings are remarkable: First, p21 levels are increased 3h after 2Gy FD-IR and second, CyclinD1 is decreased 3h after 6Gy SD-IR. Cell cycle arrest after cellular damage is classically mediated through p21 induction [23]. Therefore, the elevation of p21 in 2Gy FD-IR can be explained in this way. To the contrary, 6Gy SD-IR show no elevated p21 after 3 hours. As the p53-mediated induction of p21 is dependent on protein synthesis, the time of three hours might be too short for protein synthesis in highly damaged cells. Ma et al., for example, showed elevated amount of p21 mRNA, which is dependent on protein synthesis, after 7Gy SD-IR in glioma cells for the first time after 6 hours [63].

Instead, CyclinD1 is reduced after 6Gy SD-IR. CyclinD1 depletion is an immediate p53-independent response to DNA damage and responsible for the quick initiation of cell cycle arrest. In contrast p53 dependent p21 accumulation is much slower and responsible for maintenance of cell cycle arrest [1]. In this context, CyclinD1 depletion can be seen as a delayed reaction in the 6Gy SD-IR group, while the 2Gy FD-IR is already accu-



mutating p21. Taken these findings together we might conclude that the initial response to cellular damage is prolonged for the SD-IR groups.

##### **Late differences in Cell cycle response**

Cell cycle analysis revealed increased S-phase for SD-IR cells and increased G2 phase for FD-IR cells between 120h and 168h after IR (Fig.5 and Fig.6). Therefore two most likely explanations are possible: Cells could either be arrested or cycling in the respective phase. In case of the latter, it is remarkable that either S (in SD-IR) or G2-phase (in FD-IR) is elevated, which could be a sign of synchronized populations. On the other hand this phenomenon is detectable at all three timepoints of measure (120h, 144h and 168h) and consequently the cycling time would have to be very close to our 24 hours measure regimen. If cells are not cycling, S-phase increase in SD-IR can either be caused by arrested S-phase cells or by partly DNA-fragmented G2/M cells undergoing cell death. In this context, elevated G2/M arrest in the FD-IR group could be interpreted as cells proceeding to cell death at an earlier stage. The delayed cell death might be due to the consecutive delivery of cell damage over a longer period of time for the FD-IR group. Rubner et al. also reported about a strong induction of G2 cell cycle arrest in T98G, U251MG and U87MG glioma cells after 5x2Gy FD-IR, 48 hours after the last fraction. In addition, no G2 phase arrest was observed for 10Gy SD-IR in T98G between 4 and 72 hours and G2 arrest in U251MG cells was observed later (after 24h) and shortened [85]. To sum it up, there are various signs that damage response is performed differently between SD-IR and FD-IR.

##### **Radiotherapy in the context of multimodal treatment**

Glioblastoma cells are highly radioresistant, as we confirmed in our experiments. The issue about optimal dosing and fractionation has led to an ongoing debate in neurocranial radiotherapy [92]. On the one hand, FD-IR with low doses is associated with sublethal cellular damage and consecutive emerging therapy resistance and enhanced cellular migratory activity [112]. On the other hand, irradiation with high doses (so called



#### 4 Discussion

hypofractionated irradiation) is linked to brain necrosis, which requires surgical intervention and impairs patient's quality of life [32] [51] [71]. In addition, irradiation of children's brains with high doses is associated with cognitive impairment [17]. Current research is addressing this issue by investigating the possibility of medical intervention to protect particular susceptible areas of the brain [84].

Consequently fractions of 2Gy have been established as a clinical standard [91]. On this basis, the repetitive activation of DDR according to FD-IR is a potential target for radiosensitization. In fact, published data by Sarcar et al. showed that WEE1 inhibition, which prevents proper cell cycle arrest, drove cells into mitotic catastrophe and cellular death [86]. Interestingly, WEE1 inhibition had only moderate effects on SD-IR cells (4Gy and 6Gy), while survival decreased dramatically for the FD-IR groups (2Gy every 24h). There are many other targets in DDR which have been examined in preclinical data, namely DNA-PKcs, [115], PPARP [9] or by ATM depletion [20]. Remarkably the authors used only "low" doses up to 6Gy SD-IR or even FD-IR regimen (2Gy repetitively) to show their results. To the contrary, the effect of radiosensitizers with a pro-apoptotic side of action, namely BCL-2 [68], XIAP [10] [35], SMAC [35], TRAIL [63], has mainly been shown for radiation doses higher than 6Gy and up to 20Gy SD-IR. Under the assumption that the authors probably used the lowest doses possible for their experiments, we might speculate that DDR-affecting sensitizers become effective at lower doses, while apoptosis enhancing sensitizers rather profit from high irradiation doses. This might be explained by a filter effect of DNA damage repair as the first step on a consecutive way from damage to cellular death. As small damage is repaired more easily by the cells, the effective quantity of cellular damage which can be potentiated by pro-apoptotic sensitizers is reduced if cells repair damage more easily in low dose FD-IR regimen. In high dose SD-IR however, DDR can not cope with massive cellular damage, and pro-apoptotic sensitizers can even enhance the apoptotic effect. This might be also an explanation for the non-additive effects on specific apoptosis of PI3-Kinase pathway inhibition by rapamycin and GDC-0941 (in combination with sunitinib respectively) together with FD-IR in our experiments (Fig.11). Although GDC-0941 and Rapamycin impede the recruitment of repair proteins by the inhibition of protein synthesis, they do not directly interfere with the process of DDR and can not enhance DNA-fragmentation of 2Gy FD-IR. In this context



it would be interesting to examine further features, for example like migration and cellular motility, of PI3-Kinase pathway and other pathways in combination with FD-IR. As a conclusion, there are many differences between SD-IR and FD-IR and caution is indicated if SD-IR is taken as a surrogate for FD-IR.

## 4.2 RIST/aRIST as multitarget chemotherapy for G35dif and U87MG

Frequent genetic alteration in the RTK/RAS/PI3K pathway should make it a rewardable target in glioblastoma therapy. With the hope of higher efficiency and fewer side effects, specific inhibitors have been trialed in glioblastoma treatment but unfortunately as monotherapy of these drugs has failed to prove advantage in treatment yet [2]. Here, multitarget therapy is a promising new approach [75]. In this work, we used GDC-0941 (Pictilisib), an inhibitor of PI3K, and Rapamycin, an inhibitor of downstream target mTOR, together with Sunitinib, a multitarget kinase inhibitor. Rapamycin/Sunitinib (R/S) and GDC-0941/Sunitinib (GDC/S) had only little effect on apoptosis itself, as DNA fragmentation was at control level, but anti-proliferative effects were visible, as cell count was reduced after treatment (Fig.10). This finding is in line with literature as many authors report about growth arrest without induction of apoptosis after dual PI3K/mTOR inhibition [66] [27].

"Classical chemotherapeutics" Irinotecan (I) and Temozolomide (T) induced cell death for our cells and especially the combination of both (I/T) revealed additional effects considering apoptosis and cell count. Preclinical in vivo experiments showed similar results and it was suggested that temozolomide would increase recruitment of topoisomerase I and thereby enhance irinotecan induced damage [49]. Though a clinical phase II trial showed only at least comparable efficiency to temozolomide alone with higher side effects [81].

Quadruple therapy (Rapamycin, Irinotecan, Sunitinib, Temozolomide (RIST) and GDC-0941, Irinotecan, Sunitinib, Temozolomide (aRIST)) had additional effects towards I/T in



G35dif considering specific apoptosis and cell count, which has been shown in vitro and in vivo for various glioblastoma cell lines [75]. In U87MG, this phenomenon is expressed to a minor extent, although aRIST induces slightly more cell death than RIST and I/T.

In addition, U87MG and G35dif cells are effected by therapy to a different extent. This phenomenon could be explained by reduced sensitivity due to different molecular susceptibility for example by increased drug efflux [39] or due to different p53 function as U87MG is wildtype p53 [50]. In addition differences between U87MG and primary G35dif continue to exist in orthotopic mouse models in which U87MG only grow encapsulated without typical local invasive cells [88].

The current success of RIST in compassionate use might also be due to its metronomically designed protocol. This regiment might counteract the strong selection pressure of continuous eradication therapy towards therapy resistant subclones, which is a main problem for therapy failure. The idea behind this so-called "Adaptive Therapy" is the maintenance of a stable chemo-sensitive tumor population, which suppresses the growth of resistant populations [34]. This leads to a disease chronifying effect of therapy. Consequently many patients had prolonged survival without complete remission of tumor mass under RIST therapy [109].

### **4.3 Effects of multitarget therapy with ionizing radiation for G35dif**

Ionizing radiation and chemotherapy remain a milestone in cancer treatment. Radiotherapy with concomitant and adjuvant temozolomide chemotherapy is currently the first line treatment in primary glioblastoma therapy [44]. As RIST/aRIST therapy has shown promising preclinical results, the combination therapy with ionizing radiation is of interest. Combination therapy with "specific inhibitors" alone (R/S and GDC/S) did not affect radiation sensitivity for DNA fragmentation (Fig.11) as described previously for U87MG glioma cells [26] [4]. In contrast, R/S and GDC/S have an impact on proliferation, as cell count was reduced after chemo - radiotherapy combination treatment significantly. This might possibly be explained by the broad influence of PI3K/AKT/mTOR pathway on pro-



#### 4 Discussion

liferation, survival and metabolism [25]. In addition, with the inhibition of cellular protein synthesis, damage repair is impeded.

"Classical chemotherapy" (temozolomide (T) and temozolomide+irinotecan (I/T)) showed no enhanced effect in specific apoptosis and cell count in combination with 3x2Gy FD-IR (Fig.11). In literature, the combination therapy of temozolomide together with IR has been investigated with different results regarding synergism: Chakravarti et al. reported about an additive effect in apoptosis after 6Gy SD-IR/100 $\mu$ mol/l temozolomide combination in primary glioma cells [18]. Kil et al. proposed an additive effect 72hours after 2GySD-IR/50 $\mu$ mol/l temozolomide, but only for immunohistochemically counted mitotic catastrophe and not for apoptosis [54]. Rubner et. al however, displayed no additional effect in T98G and U251MG cells and only a marginal but statistically significant effect in U87MG [85]. Remarkably, in this publication a 5x2Gy FD-IR regimen is applied and the author reported about an increased late apoptosis upon FD-IR. As published data for temozolomide/IR combination is inconsistent, temozolomide and IR combination therapy can at best be described as additive [55] [8] [105]. In clinical trials, temozolomide and radiotherapy showed an enhanced median survival about 2.5 months and a doubled 2-year survival rate towards radiotherapy alone [98].

A slight reduction in DNA fragmentation for IR+chemotherapy in our cells might be explained by various reasons: FD-IR irradiated cells were kept in a repetitive state of DNA repair which might counteract chemotherapy or at least prolong the induction of cell death. Here, measurements at a later time or colony formation would help to examine longlasting effects. In addition, as described previously, delayed cell death might play a role in G35dif cells and an assay for mitotic catastrophe (e.g. video microscopy [82]) is auspicious for prospective experimentation. Furthermore, chemotherapeutic drugs which interfere with DNA replication profit from fast dividing cells because of increased chromosomal breaks. Therefore cell cycle arrest due to specific inhibitors and radiotherapy might delay the effect of chemotherapy.

In addition, we could show the onset of Rapamycin/Sunitinib combination is between 15min and 60min while GDC-0941/Sunitinib affects cells between 1h and 4h (Fig.12).



#### *4 Discussion*

As cells were irradiated without extra incubation time, some cells (the first stimulated ones) might already be affected by treatment while others were not. This might also account for high error bars in this experiment. In order to provide equal conditions for all groups, a sufficient incubation time (e.g. 24 hours) is recommendable for further experimentation. Moreover, these experiments should be validated with different tumor cells like G38dif or other commercial glioblastoma cell lines. Also, the experimental setting could be extended to a 5x2Gy FD-IR scheme in which the effect of radiation is intensified as described.

Taken together, no additional effect in specific apoptosis and cell count was observed after 120 hours for radio-chemotherapy with the used assay. Though, multiple target therapy is a potential new therapeutic option in glioblastoma therapy. Implementation into irradiation regimes will therefore highly depend on suitable drug-irradiation schedules. As we displayed the importance of clinically relevant regimes in preclinical settings, this should also be taken into account for radio-chemo combination therapy.



## 5 Summary

In this work we examined the effect of irradiation on primary differentiated glioblastoma tumor cells, and characterized them in terms of radiobiologic parameters. We found that irradiation caused inhibition of colony formation and altered cellular morphology depending on irradiation dose. Further, we examined the differences between Single Dose Irradiation (SD-IR) and clinically relevant Fractionated Dose Irradiation (FD-IR). For high irradiation doses (10Gy), SD-IR caused more cell damage than 5x2Gy FD-IR. Regarding 3x2Gy FD-IR versus 6Gy SD-IR we noticed no differences in cell number and DNA-fragmentation but differences in DNA Damage Response (DDR). Here, we could show the repetitive activation of DNA damage response after FD-IR in direct comparison to SD-IR. While SD-IR activates DDR signaling only once, FD-IR cells are kept in a repetitive active state of DNA damage repair, which might be an explanation for reduced cellular damage after FD-IR. Considering these findings we can state that FD-IR mimics the clinical effects better than SD-IR and therefore it is the model of choice for future experiments.

In a next step we included FD-IR into a multitarget therapy regimen, consisting of specific inhibition of aberrant PI3-Kinase pathway and chemotherapy. Here, higher rates of specific apoptosis and less cell count was detected when chemotherapy was applied together with specific pathway inhibitors than alone. In combination with FD-IR, specific inhibitors showed less cell count. For chemotherapy or multitarget therapy antagonistic effects could be provoked in combination with FD-IR, which warrants further investigation.

In summary we established an irradiation protocol with Fractionated Dose Irradiation (FD-IR) on the basis of clinically relevant doses and applied it to a multitarget therapy.



## 6 Bibliography

- [1] AGAMI, R., AND BERNARDS, R. Distinct initiation and maintenance mechanisms cooperate to induce g1 cell cycle arrest in response to dna damage. *Cell* 102 (2000), 55–66.
- [2] AKHAVAN, D., CLOUGHESY, T. F., AND MISCHER, P. S. mtor signaling in glioblastoma: lessons learned from bench to bedside. *Neuro Oncol* 12 (2010), 882–889.
- [3] ALPHONSE, G., MAALOUF, M., BATTISTON-MONTAGNE, P., ARDAIL, D., BEUVE, M., ROUSSON, R., TAUCHER-SCHOLZ, G., FOURNIER, C., AND RODRIGUEZ-LAFRASSE, C. p53-independent early and late apoptosis is mediated by ceramide after exposure of tumor cells to photon or carbon ion irradiation. *BMC Cancer* 13 (2013), 151.
- [4] ANANDHARAJ, A., CINGHU, S., AND PARK, W.-Y. Rapamycin-mediated mtor inhibition attenuates survivin and sensitizes glioblastoma cells to radiation therapy. *Acta Biochim Biophys Sin (Shanghai)* 43 (2011), 292–300.
- [5] AZZAM, E. I., JAY-GERIN, J.-P., AND PAIN, D. Ionizing radiation-induced metabolic oxidative stress and prolonged cell injury. *Cancer Lett* 327 (2012), 48–60.
- [6] BALBOUS, A., CORTES, U., GUILLOTEAU, K., RIVET, P., PINEL, B., DUCHESNE, M., GODET, J., BOISSONNADE, O., WAGER, M., BENSADOUN, R. J., CHOMEL, J.-C., AND KARAYAN-TAPON, L. A radiosensitizing effect of rad51 inhibition in glioblastoma stem-like cells. *BMC cancer* 16 (2016), 604.
- [7] BAO, S., WU, Q., MCLENDON, R. E., HAO, Y., SHI, Q., HJELMELAND, A. B., DEWHIRST, M. W., BIGNER, D. D., AND RICH, J. N. Glioma stem cells promote radioresistance by preferential activation of the dna damage response. *Nature* 444 (2006), 756–760.
- [8] BARAZZUOL, L., JENA, R., BURNET, N. G., JEYNES, J. C. G., MERCHANT, M. J., KIRKBY, K. J., AND KIRKBY, N. F. In vitro evaluation of combined temozolomide



## 6 Bibliography

- and radiotherapy using x rays and high-linear energy transfer radiation for glioblastoma. *Radiat Res* 177 (2012), 651–662.
- [9] BARAZZUOL, L., JENA, R., BURNET, N. G., MEIRA, L. B., JEYNES, J. C. G., KIRKBY, K. J., AND KIRKBY, N. F. Evaluation of poly (adp-ribose) polymerase inhibitor abt-888 combined with radiotherapy and temozolomide in glioblastoma. *Radiat Oncol* 8 (2013), 65.
- [10] BERGER, R., JENNEWEIN, C., MARSCHALL, V., KARL, S., CRISTOFANON, S., WAGNER, L., VELLANKI, S. H., HEHLGANS, S., RÖDEL, F., DEBATIN, K.-M., LUDOLPH, A. C., AND FULDA, S. Nf- $\kappa$ b is required for smac mimetic-mediated sensitization of glioblastoma cells for  $\gamma$ -irradiation-induced apoptosis. *Mol Cancer Ther* 10 (2011), 1867–1875.
- [11] BERNIER, J., HALL, E. J., AND GIACCIA, A. Radiation oncology: a century of achievements. *Nat Rev Cancer* 4 (2004), 737–747.
- [12] BLISS, C. I. The toxicity of poisons applied jointly. *Annals of Applied Biology* 26 (1939), 585–615.
- [13] BLUME-JENSEN, P., AND HUNTER, T. Oncogenic kinase signalling. *Nature* 411 (2001), 355–365.
- [14] BROWN, J. M., AND ATTARDI, L. D. The role of apoptosis in cancer development and treatment response. *Nat Rev Cancer* 5 (2005), 231–237.
- [15] CADENAS, E., AND DAVIES, K. J. Mitochondrial free radical generation, oxidative stress, and aging. *Free Radic Biol Med* 29 (2000), 222–230.
- [16] CADWELL, C., AND ZAMBETTI, G. P. The effects of wild-type p53 tumor suppressor activity and mutant p53 gain-of-function on cell growth. *Gene* 277 (2001), 15–30.
- [17] CARRIE, C., MURACCIOLE, X., GOMEZ, F., HABRAND, J.-L., BENHASSEL, M., MEGE, M., MAHÉ, M., QUETIN, P., MAIRE, J. P., SOUM, F., BARON, M. H., CLAVERE, P., CHAPET, S., GACI, Z., KOLODIE, H., MAINGON, P., VIE, B., BERNIER, V., ALAPETITE, C., HOFFSTETTER, S., GRILL, J., LAFAY, F., AND OF PEDI-  
ATRIC ONCOLOGY, F. S. Conformal radiotherapy, reduced boost volume, hyper-



## 6 Bibliography

- fractionated radiotherapy, and online quality control in standard-risk medulloblastoma without chemotherapy: results of the french m-sfop 98 protocol. *International journal of radiation oncology, biology, physics* 63 (2005), 711–716.
- [18] CHAKRAVARTI, A., ERKKINEN, M. G., NESTLER, U., STUPP, R., MEHTA, M., AL-DAPE, K., GILBERT, M. R., BLACK, P. M., AND LOEFFLER, J. S. Temozolomide-mediated radiation enhancement in glioblastoma: a report on underlying mechanisms. *Clin Cancer Res* 12 (2006), 4738–4746.
- [19] CHOI, E. K., LEE, Y. H., CHOI, Y. S., KWON, H. M., CHOI, M. S., RO, J. Y., PARK, S.-K., AND YU, E. Heterogeneous expression of ku70 in human tissues is associated with morphological and functional alterations of the nucleus. *J Pathol* 198 (2002), 121–130.
- [20] CHUAH, T. L., WALKER, D. G., WEI, M., SCOTT, S., AND LAVIN, M. F. Approaches to sensitizing glioblastoma to radiotherapy: use of lentiviral vectors. *Int J Oncol* 40 (2012), 1963–1969.
- [21] CORDES, N., HANSMEIER, B., BEINKE, C., MEINEKE, V., AND VAN BEUNINGEN, D. Irradiation differentially affects substratum-dependent survival, adhesion, and invasion of glioblastoma cell lines. *Br J Cancer* 89 (2003), 2122–2132.
- [22] DARZYNKIEWICZ, Z., TRAGANOS, F., ZHAO, H., HALICKA, H. D., SKOMMER, J., AND WLODKOWIC, D. Analysis of individual molecular events of dna damage response by flow- and image-assisted cytometry. *Methods Cell Biol* 103 (2011), 115–147.
- [23] DULIĆ, V., STEIN, G. H., FAR, D. F., AND REED, S. I. Nuclear accumulation of p21cip1 at the onset of mitosis: a role at the g2/m-phase transition. *Mol Cell Biol* 18, 1 (1998), 546–557.
- [24] EDINGER, A. L., AND THOMPSON, C. B. Death by design: apoptosis, necrosis and autophagy. *Curr Opin Cell Biol* 16 (2004), 663–669.
- [25] ERSAHIN, T., TUNCBAG, N., AND CETIN-ATALAY, R. The pi3k/akt/mtor interactive pathway. *Mol Biosyst* (2015), 1946–54.



## 6 Bibliography

- [26] ESHLEMAN, J. S., CARLSON, B. L., MLADEK, A. C., KASTNER, B. D., SHIDE, K. L., AND SARKARIA, J. N. Inhibition of the mammalian target of rapamycin sensitizes u87 xenografts to fractionated radiation therapy. *Cancer Res* 62 (2002), 7291–7297.
- [27] FAN, Q.-W., KNIGHT, Z. A., GOLDENBERG, D. D., YU, W., MOSTOV, K. E., STOKOE, D., SHOKAT, K. M., AND WEISS, W. A. A dual pi3 kinase/mtor inhibitor reveals emergent efficacy in glioma. *Cancer Cell* 9 (2006), 341–349.
- [28] FELL, V. L., AND SCHILD-POULTER, C. The ku heterodimer: function in dna repair and beyond. *Mutat Res Rev Mutat Res* 763 (2015), 15–29.
- [29] FERTIL, B., AND MALAISE, E. P. Inherent cellular radiosensitivity as a basic concept for human tumor radiotherapy. *International journal of radiation oncology, biology, physics* 7 (1981), 621–629.
- [30] FIRAT, E., GAEDICKE, S., TSURUMI, C., ESSER, N., WEYERBROCK, A., AND NIEDERMANN, G. Delayed cell death associated with mitotic catastrophe in  $\gamma$ -irradiated stem-like glioma cells. *Radiat Oncol* 6 (2011), 71.
- [31] FLAMAN, J. M., FREBOURG, T., MOREAU, V., CHARBONNIER, F., MARTIN, C., CHAPPUIS, P., SAPPINO, A. P., LIMACHER, I. M., BRON, L., AND BENHATTAR, J. A simple p53 functional assay for screening cell lines, blood, and tumors. *Proc Natl Acad Sci U S A* 92 (1995), 3963–3967.
- [32] FLOYD, N. S., WOO, S. Y., TEH, B. S., PRADO, C., MAI, W.-Y., TRASK, T., GILDENBERG, P. L., HOLOYE, P., AUGSPURGER, M. E., CARPENTER, L. S., LU, H. H., CHIU, J. K., GRANT, W. H., AND BUTLER, E. B. Hypofractionated intensity-modulated radiotherapy for primary glioblastoma multiforme. *International journal of radiation oncology, biology, physics* 58 (2004), 721–726.
- [33] FOWLER, J. F. The linear-quadratic formula and progress in fractionated radiotherapy. *Br J Radiol* 62 (1989), 679–694.
- [34] GATENBY, R. A., SILVA, A. S., GILLIES, R. J., AND FRIEDEN, B. R. Adaptive therapy. *Cancer Res* 69 (2009), 4894–4903.



## 6 Bibliography

- [35] GIAGKOUSIKLIDIS, S., VOGLER, M., WESTHOFF, M.-A., KASPERCZYK, H., DEBATIN, K.-M., AND FULDA, S. Sensitization for gamma-irradiation-induced apoptosis by second mitochondria-derived activator of caspase. *Cancer Res* 65 (2005), 10502–10513.
- [36] GOLSTEIN, P., AND KROEMER, G. Cell death by necrosis: towards a molecular definition. *Trends Biochem Sci* 32 (2007), 37–43.
- [37] GRUNERT, M., KASSUBEK, R., DANZ, B., KLEMENZ, B., HASSLACHER, S., STROH, S., SCHNEELE, L., LANGHANS, J., STRÖBELE, S., BARRY, S. E., ZHOU, S., DEBATIN, K.-M., AND WESTHOFF, M.-A. Radiation and brain tumors: An overview. *Critical reviews in oncogenesis* 23 (2018), 119–138.
- [38] HAAKE, A. R., AND POLAKOWSKA, R. R. Cell death by apoptosis in epidermal biology. *J Invest Dermatol* 101 (1993), 107–112.
- [39] HAAR, C. P., HEBBAR, P., WALLACE, 4TH, G. C., DAS, A., VANDERGRIFT, 3RD, W. A., SMITH, J. A., GIGLIO, P., PATEL, S. J., RAY, S. K., AND BANIK, N. L. Drug resistance in glioblastoma: a mini review. *Neurochem Res* 37 (2012), 1192–1200.
- [40] HALL, E., AND GIACCIA, A. *Radiobiology for the Radiologist, 7th ed.* Lippincott, Williams & Wilkins, Philadelphia, USA, 2012.
- [41] HALL, J. S., IYPE, R., SENRA, J., TAYLOR, J., ARMENOULT, L., OGUEJIOFOR, K., LI, Y., STRATFORD, I., STERN, P. L., O’CONNOR, M. J., MILLER, C. J., AND WEST, C. M. L. Investigation of radiosensitivity gene signatures in cancer cell lines. *PLoS One* 9 (2014), e86329.
- [42] HANAHAN, D., AND WEINBERG, R. A. The hallmarks of cancer. *Cell* 100 (2000), 57–70.
- [43] HANAHAN, D., AND WEINBERG, R. A. Hallmarks of cancer: the next generation. *Cell* 144 (2011), 646–674.
- [44] HART, M. G., GARSIDE, R., ROGERS, G., STEIN, K., AND GRANT, R. Temozolomide for high grade glioma. *Cochrane Database Syst Rev* 4 (2013), CD007415.



## 6 Bibliography

- [45] HASSLACHER, S., SCHNEELE, L., STROH, S., LANGHANS, J., ZEILER, K., KAT-  
TNER, P., KARPEL-MASSLER, G., SIEGELIN, M. D., SCHNEIDER, M., ZHOU, S.,  
GRUNERT, M., HALATSCH, M.-E., NONNENMACHER, L., DEBATIN, K.-M., AND  
WESTHOFF, M.-A. Inhibition of pi3k signalling increases the efficiency of radio-  
therapy in glioblastoma cells. *International journal of oncology* 53 (2018), 1881–  
1896.
- [46] HAUSMANN, C., TEMME, A., CORDES, N., AND EKE, I. Ilkap, ilk and pinch1  
control cell survival of p53-wildtype glioblastoma cells after irradiation. *Oncotarget*  
6 (2015), 34592–34605.
- [47] HEGI, M. E., DISERENS, A.-C., GODARD, S., DIETRICH, P.-Y., REGLI, L., OS-  
TERMANN, S., OTTEN, P., VAN MELLE, G., DE TRIBOLET, N., AND STUPP, R.  
Clinical trial substantiates the predictive value of o-6-methylguanine-dna methyl-  
transferase promoter methylation in glioblastoma patients treated with temozolo-  
mide. *Clin Cancer Res* 10 (2004), 1871–1874.
- [48] HENGARTNER, M. O. The biochemistry of apoptosis. *Nature* 407 (2000), 770–  
776.
- [49] HOUGHTON, P. J., STEWART, C. F., CHESHIRE, P. J., RICHMOND, L. B.,  
KIRSTEIN, M. N., POQUETTE, C. A., TAN, M., FRIEDMAN, H. S., AND BRENT,  
T. P. Antitumor activity of temozolomide combined with irinotecan is partly inde-  
pendent of o6-methylguanine-dna methyltransferase and mismatch repair pheno-  
types in xenograft models. *Clin Cancer Res* 6 (2000), 4110–4118.
- [50] ISHII, N., MAIER, D., MERLO, A., TADA, M., SAWAMURA, Y., DISERENS, A. C.,  
AND VAN MEIR, E. G. Frequent co-alterations of tp53, p16/cdkn2a, p14arf, pten  
tumor suppressor genes in human glioma cell lines. *Brain Pathol* 9 (1999), 469–  
479.
- [51] IUCHI, T., HATANO, K., KODAMA, T., SAKAIDA, T., YOKOI, S., KAWASAKI, K.,  
HASEGAWA, Y., AND HARA, R. Phase 2 trial of hypofractionated high-dose inten-  
sity modulated radiation therapy with concurrent and adjuvant temozolomide for



## 6 Bibliography

- newly diagnosed glioblastoma. *International journal of radiation oncology, biology, physics* 88 (2014), 793–800.
- [52] JIANG, Z., PORE, N., CERNIGLIA, G. J., MICK, R., GEORGESCU, M.-M., BERNHARD, E. J., HAHN, S. M., GUPTA, A. K., AND MAITY, A. Phosphatase and tensin homologue deficiency in glioblastoma confers resistance to radiation and temozolomide that is reversed by the protease inhibitor nelfinavir. *Cancer research* 67 (2007), 4467–4473.
- [53] KAATSCH P, S. C. German childhood cancer registry - report 2012 (1980-2012). *Institute of Medical Biostatistics, Epidemiology and Informatics (IMBEI) at the University Medical Center of the Johannes Gutenberg University Mainz* (2013).
- [54] KIL, W. J., CERNA, D., BURGAN, W. E., BEAM, K., CARTER, D., STEEG, P. S., TOFILON, P. J., AND CAMPHAUSEN, K. In vitro and in vivo radiosensitization induced by the dna methylating agent temozolomide. *Clin Cancer Res* 14 (2008), 931–938.
- [55] KOUKOURAKIS, G. V., KOULOULIAS, V., ZACHARIAS, G., PAPADIMITRIOU, C., PANTELAKOS, P., MARAVELIS, G., FOTINEAS, A., BELI, I., CHALDEOPOULOS, D., AND KOUVARIS, J. Temozolomide with radiation therapy in high grade brain gliomas: pharmaceutical considerations and efficacy; a review article. *Molecules* 14 (2009), 1561–1577.
- [56] KROEMER, G., GALLUZZI, L., VANDENABEELE, P., ABRAMS, J., ALNEMRI, E. S., BAEHRECKE, E. H., BLAGOSKLONNY, M. V., EL-DEIRY, W. S., GOLSTEIN, P., GREEN, D. R., HENGARTNER, M., KNIGHT, R. A., KUMAR, S., LIPTON, S. A., MALORNI, W., NUNEZ, G., PETER, M. E., TSCHOPP, J., YUAN, J., PIACENTINI, M., ZHIVOTOVSKY, B., MELINO, G., AND , N. C. O. C. D. . Classification of cell death: recommendations of the nomenclature committee on cell death 2009. *Cell Death Differ* 16 (2009), 3–11.
- [57] KUGER, S., FLENTJE, M., AND DJUZENOVA, C. S. Simultaneous perturbation of the mapk and the pi3k/mtor pathways does not lead to increased radiosensitization. *Radiation oncology* 10 (2015), 214.



## 6 Bibliography

- [58] LI, N., MALY, D. J., CHANTHERY, Y. H., SIRKIS, D. W., NAKAMURA, J. L., BERGER, M. S., JAMES, C. D., SHOKAT, K. M., WEISS, W. A., AND PERSSON, A. I. Radiotherapy followed by aurora kinase inhibition targets tumor-propagating cells in human glioblastoma. *Molecular cancer therapeutics* 14 (2015), 419–428.
- [59] LISBY, M., AND ROTHSTEIN, R. Choreography of recombination proteins during the dna damage response. *DNA Repair* 8 (2009), 1068–1076.
- [60] LIU, Y.-J., LIN, Y.-F., CHEN, Y.-F., LUO, E.-C., SHER, Y.-P., TSAI, M.-H., CHUANG, E. Y., AND LAI, L.-C. Microrna-449a enhances radiosensitivity in cl1-0 lung adenocarcinoma cells. *PLoS One* 8 (2013), e62383.
- [61] LOUIS, D. N., POMEROY, S. L., AND CAIRNCROSS, J. G. Focus on central nervous system neoplasia. *Cancer Cell* 1 (2002), 125–128.
- [62] LUKAS, J., LUKAS, C., AND BARTEK, J. More than just a focus: The chromatin response to dna damage and its role in genome integrity maintenance. *Nat Cell Biol* 13 (2011), 1161–1169.
- [63] MA, H., RAO, L., WANG, H. L., MAO, Z. W., LEI, R. H., YANG, Z. Y., QING, H., AND DENG, Y. L. Transcriptome analysis of glioma cells for the dynamic response to  $\gamma$ -irradiation and dual regulation of apoptosis genes: a new insight into radiotherapy for glioblastomas. *Cell Death Dis* 4 (2013), e895.
- [64] MA, Y., PANNICKE, U., SCHWARZ, K., AND LIEBER, M. R. Hairpin opening and overhang processing by an artemis/dna-dependent protein kinase complex in non-homologous end joining and v(d)j recombination. *Cell* 108 (2002), 781–794.
- [65] MAHANEY, B. L., MEEK, K., AND LEES-MILLER, S. P. Repair of ionizing radiation-induced dna double-strand breaks by non-homologous end-joining. *Biochem J* 417 (2009), 639–650.
- [66] MAIRA, S.-M., STAUFFER, F., BRUEGGEN, J., FURET, P., SCHNELL, C., FRITSCH, C., BRACHMANN, S., CHÈNE, P., DE POVER, A., SCHOEMAKER, K., FABBRO, D., GABRIEL, D., SIMONEN, M., MURPHY, L., FINAN, P., SELLERS, W., AND GARCÍA-ECHEVERRÍA, C. Identification and characterization of nvp-bez235, a new orally available dual phosphatidylinositol 3-kinase/mammalian target of ra-



## 6 Bibliography

- pamycin inhibitor with potent in vivo antitumor activity. *Mol Cancer Ther* 7 (2008), 1851–1863.
- [67] MAZURIK, V. K., AND MOROZ, B. B. Problems of radiobiology and p53 protein. *Radiats Biol Radioecol* 41 (2001), 548–572.
- [68] MORETTI, L., LI, B., KIM, K. W., CHEN, H., AND LU, B. At-101, a pan-bcl-2 inhibitor, leads to radiosensitization of non-small cell lung cancer. *J Thorac Oncol* 5 (2010), 680–687.
- [69] MUKHERJEE, B., TOMIMATSU, N., AMANCHERLA, K., CAMACHO, C. V., PICHAMOORTHY, N., AND BURMA, S. The dual pi3k/mTOR inhibitor nvp-bez235 is a potent inhibitor of ATM- and DNA-PKcs-mediated DNA damage responses. *Neoplasia* 14 (2012), 34–43.
- [70] NETWORK, T. C. G. A. T. R. Comprehensive genomic characterization defines human glioblastoma genes and core pathways. *Nature* 455 (2008), 1061–1068.
- [71] NEY, D. E., CARLSON, J. A., DAMEK, D. M., GASPAR, L. E., KAVANAGH, B. D., KLEINSCHMIDT-DEMASTERS, B. K., WAZIRI, A. E., LILLEHEI, K. O., REDDY, K., AND CHEN, C. Phase II trial of hypofractionated intensity-modulated radiation therapy combined with temozolomide and bevacizumab for patients with newly diagnosed glioblastoma. *Journal of neuro-oncology* 122 (2015), 135–143.
- [72] NICOLETTI, I., MIGLIORATI, G., PAGLIACCI, M. C., GRIGNANI, F., AND RICCARDI, C. A rapid and simple method for measuring thymocyte apoptosis by propidium iodide staining and flow cytometry. *J Immunol Methods* 139 (1991), 271–279.
- [73] NILSSON, S., CARLSSON, J., LARSSON, B., AND PONTEN, J. Survival of irradiated glia and glioma cells studied with a new cloning technique. *International journal of radiation biology and related studies in physics, chemistry, and medicine* 37 (1980), 267–279.
- [74] NONNENMACHER, L., HASSLACHER, S., ZIMMERMANN, J., KARPEL-MASSLER, G., LA FERLA-BRÜHL, K., BARRY, S. E., BURSTER, T., SIEGELIN, M. D., BRÜHL, O., HALATSCH, M.-E., DEBATIN, K.-M., AND WESTHOFF, M.-A. Cell death induc-



## 6 Bibliography

- tion in cancer therapy - past, present, and future. *Critical reviews in oncogenesis* 21 (2016), 253–267.
- [75] NONNENMACHER, L., WESTHOFF, M.-A., FULDA, S., KARPEL-MASSLER, G., HALATSCH, M.-E., ENGELKE, J., SIMMET, T., CORBACIOGLU, S., AND DEBATIN, K.-M. Rist: a potent new combination therapy for glioblastoma. *International journal of cancer* 136 (2015), E173–E187.
- [76] O'DRISCOLL, M., AND JEGGO, P. A. The role of double-strand break repair - insights from human genetics. *Nat Rev Genet* 7 (2006), 45–54.
- [77] OHGAKI, H., AND KLEIHUES, P. Population-based studies on incidence, survival rates, and genetic alterations in astrocytic and oligodendroglial gliomas. *J Neuropathol Exp Neurol* 64 (2005), 479–489.
- [78] OSTROM, Q. T., GITTLEMAN, H., FARAH, P., ONDRACEK, A., CHEN, Y., WOLINSKY, Y., STROUP, N. E., KRUCHKO, C., AND BARNHOLTZ-SLOAN, J. S. Cbtrus statistical report: Primary brain and central nervous system tumors diagnosed in the united states in 2006-2010. *Neuro Oncol* 15 Suppl 2 (2013), ii1–i56.
- [79] PAN, E., YU, D., YUE, B., POTTHAST, L., CHOWDHARY, S., SMITH, P., AND CHAMBERLAIN, M. A prospective phase ii single-institution trial of sunitinib for recurrent malignant glioma. *J Neurooncol* 110 (2012), 111–118.
- [80] PETKAU, A. Role of superoxide dismutase in modification of radiation injury. *Br J Cancer Suppl* 8 (1987), 87–95.
- [81] QUINN, J. A., JIANG, S. X., REARDON, D. A., DESJARDINS, A., VREDENBURGH, J. J., FRIEDMAN, A. H., SAMPSON, J. H., MCLENDON, R. E., HERNDON, 2ND, J. E., AND FRIEDMAN, H. S. Phase ii trial of temozolomide (tmz) plus irinotecan (cpt-11) in adults with newly diagnosed glioblastoma multiforme before radiotherapy. *J Neurooncol* 95 (2009), 393–400.
- [82] RELLO-VARONA, S., KEPP, O., VITALE, I., MICHAUD, M., SENOVILLA, L., JEMAÀ, M., JOZA, N., GALLUZZI, L., CASTEDO, M., AND KROEMER, G. An automated fluorescence videomicroscopy assay for the detection of mitotic catastrophe. *Cell Death Dis* 1 (2010), e25.



## 6 Bibliography

- [83] RONINSON, I. B., BROUDE, E. V., AND CHANG, B. D. If not apoptosis, then what? treatment-induced senescence and mitotic catastrophe in tumor cells. *Drug Resist Updat* 4 (2001), 303–313.
- [84] ROONEY, J. W., AND LAACK, N. N. Pharmacological interventions to treat or prevent neurocognitive decline after brain radiation. *CNS oncology* (2013), 531–541.
- [85] RUBNER, Y., MUTH, C., STRNAD, A., DERER, A., SIEBER, R., BUSLEI, R., FREY, B., FIETKAU, R., AND GAIP, U. S. Fractionated radiotherapy is the main stimulus for the induction of cell death and of hsp70 release of p53 mutated glioblastoma cell lines. *Radiat Oncol* 9 (2014), 89.
- [86] SARGAR, B., KAHALI, S., PRABHU, A. H., SHUMWAY, S. D., XU, Y., DEMUTH, T., AND CHINNAIAN, P. Targeting radiation-induced g(2) checkpoint activation with the wee-1 inhibitor mk-1775 in glioblastoma cell lines. *Mol Cancer Ther* 10 (2011), 2405–2414.
- [87] SARKER, D., ANG, J. E., BAIRD, R., KRISTELEIT, R., SHAH, K., MORENO, V., CLARKE, P. A., RAYNAUD, F. I., LEVY, G., WARE, J. A., MAZINA, K., LIN, R., WU, J., FREDRICKSON, J., SPOERKE, J. M., LACKNER, M. R., YAN, Y., FRIEDMAN, L. S., KAYE, S. B., DERYNCK, M. K., WORKMAN, P., AND DE BONO, J. S. First-in-human phase i study of pictilisib (gdc-0941), a potent pan-class i phosphatidylinositol-3-kinase (pi3k) inhibitor, in patients with advanced solid tumors. *Clin Cancer Res* 21 (2015), 77–86.
- [88] SCHNEIDER, M., STRÖBELE, S., NONNENMACHER, L., SIEGELIN, M. D., TEPPER, M., STROH, S., HASSLACHER, S., ENZENMÜLLER, S., STRAUSS, G., BAUMANN, B., KARPEL-MASSLER, G., WESTHOFF, M.-A., DEBATIN, K.-M., AND HALATSCH, M.-E. A paired comparison between glioblastoma "stem cells" and differentiated cells. *International journal of cancer* 138 (2016), 1709–1718.
- [89] SCHRECK, K. C., AND GROSSMAN, S. A. Role of temozolomide in the treatment of cancers involving the central nervous system. *Oncology* 32 (2018), 555–60, 569.



## 6 Bibliography

- [90] SETUA, S., OUBERAI, M., PICCIRILLO, S. G., WATTS, C., AND WELLAND, M. Cisplatin-tethered gold nanospheres for multimodal chemo-radiotherapy of glioblastoma. *Nanoscale* 6 (2014), 10865–10873.
- [91] SHELINE, G. E. Radiotherapy for high grade gliomas. *International journal of radiation oncology, biology, physics* 18 (1990), 793–803.
- [92] SHIBAMOTO, Y., MIYAKAWA, A., OTSUKA, S., AND IWATA, H. Radiobiology of hypofractionated stereotactic radiotherapy: what are the optimal fractionation schedules? *Journal of radiation research* 57 (2016), i76–i82.
- [93] SHILOH, Y. The atm-mediated dna-damage response: taking shape. *Trends Biochem Sci* 31 (2006), 402–410.
- [94] SHIN, J.-I., SHIM, J.-H., KIM, K.-H., CHOI, H.-S., KIM, J.-W., LEE, H.-G., KIM, B.-Y., PARK, S.-N., PARK, O.-J., AND YOON, D.-Y. Sensitization of the apoptotic effect of gamma-irradiation in genistein-pretreated caski cervical cancer cells. *J Microbiol Biotechnol* 18 (2008), 523–531.
- [95] SHORT, S. C., MARTINDALE, C., BOURNE, S., BRAND, G., WOODCOCK, M., AND JOHNSTON, P. Dna repair after irradiation in glioma cells and normal human astrocytes. *Neuro Oncol* 9 (2007), 404–411.
- [96] SIZOO, E. M., BRAAM, L., POSTMA, T. J., PASMAN, H. R. W., HEIMANS, J. J., KLEIN, M., REIJNEVELD, J. C., AND TAPHOORN, M. J. B. Symptoms and problems in the end-of-life phase of high-grade glioma patients. *Neuro Oncol* 12 (2010), 1162–1166.
- [97] SPITZ, D. R., AZZAM, E. I., LI, J. J., AND GIUS, D. Metabolic oxidation/reduction reactions and cellular responses to ionizing radiation: a unifying concept in stress response biology. *Cancer Metastasis Rev* 23 (2004), 311–322.
- [98] STUPP, R., MASON, W. P., VAN DEN BENT, M. J., WELLER, M., FISHER, B., TAPHOORN, M. J. B., BELANGER, K., BRANDES, A. A., MAROSI, C., BOGDahn, U., CURSCHMANN, J., JANZER, R. C., LUDWIN, S. K., GORLIA, T., ALLGEIER, A., LACOMBE, D., CAIRNCROSS, J. G., EISENHAEUER, E., MIRIMANOFF, R. O., , E. O. F. R., OF CANCER BRAIN TUMOR, T., GROUPS, R., AND , N. C. I. O. C. C.



## 6 Bibliography

- T. G. Radiotherapy plus concomitant and adjuvant temozolomide for glioblastoma. *N Engl J Med* 352 (2005), 987–996.
- [99] TAGHIAN, A., SUIT, H., PARDO, F., GIOIOSO, D., TOMKINSON, K., DUBOIS, W., AND GERWECK, L. In vitro intrinsic radiation sensitivity of glioblastoma multiforme. *Int J Radiat Oncol Biol Phys* 23 (1992), 55–62.
- [100] TAKAHASHI, A., AND OHNISHI, T. Does gamma<sup>2</sup>ax foci formation depend on the presence of dna double strand breaks? *Cancer Lett* 229 (2005), 171–179.
- [101] THOMPSON, L. H. Recognition, signaling, and repair of dna double-strand breaks produced by ionizing radiation in mammalian cells: the molecular choreography. *Mutat Res* 751 (2012), 158–246.
- [102] VAKIFAHMETOGLU, H., OLSSON, M., AND ZHIVOTOVSKY, B. Death through a tragedy: mitotic catastrophe. *Cell Death Differ* 15 (2008), 1153–1162.
- [103] VOGELSTEIN, B., LANE, D., AND LEVINE, A. J. Surfing the p53 network. *Nature* 408 (2000), 307–310.
- [104] WANG, P., ZHEN, H., JIANG, X., ZHANG, W., CHENG, X., GUO, G., MAO, X., AND ZHANG, X. Boron neutron capture therapy induces apoptosis of glioma cells through bcl-2/bax. *BMC cancer* 10 (2010), 661.
- [105] WEDGE, S. R., PORTEOUS, J. K., GLASER, M. G., MARCUS, K., AND NEWLANDS, E. S. In vitro evaluation of temozolomide combined with x-irradiation. *Anticancer Drugs* 8 (1997), 92–97.
- [106] WEINBERG, R. A. *The Biology of Cancer*. Garland Science, Taylor&Francis Group, LLC, 2007.
- [107] WELSH, J. W., MAHADEVAN, D., ELLSWORTH, R., COOKE, L., BEARSS, D., AND STEA, B. The c-met receptor tyrosine kinase inhibitor mp470 radiosensitizes glioblastoma cells. *Radiation oncology* 4 (2009), 69.
- [108] WEN, P. Y., AND KESARI, S. Malignant gliomas in adults. *N Engl J Med* 359 (2008), 492–507.



## 6 Bibliography

- [109] WESTHOFF, M.-A., BRÜHL, O., NONNENMACHER, L., KARPEL-MASSLER, G., AND DEBATIN, K.-M. Killing me softly–future challenges in apoptosis research. *Int J Mol Sci* 15 (2014), 3746–3767.
- [110] WESTHOFF, M.-A., ZHOU, S., NONNENMACHER, L., KARPEL-MASSLER, G., JENNEWEIN, C., SCHNEIDER, M., HALATSCH, M.-E., CARRAGHER, N. O., BAUMANN, B., KRAUSE, A., SIMMET, T., BACHEM, M. G., WIRTZ, C. R., AND DEBATIN, K.-M. Inhibition of nf- $\kappa$ b signaling ablates the invasive phenotype of glioblastoma. *Mol Cancer Res* 11 (2013), 1611–1623.
- [111] WICK, W., WELLER, M., WEILER, M., BATCHELOR, T., YUNG, A. W. K., AND PLATTEN, M. Pathway inhibition: emerging molecular targets for treating glioblastoma. *Neuro Oncol* 13 (2011), 566–579.
- [112] WILD-BODE, C., WELLER, M., RIMNER, A., DICHGANS, J., AND WICK, W. Sublethal irradiation promotes migration and invasiveness of glioma cells: implications for radiotherapy of human glioblastoma. *Cancer research* 61 (2001), 2744–2750.
- [113] WILLIAMS, J. R., ZHANG, Y., ZHOU, H., GRIDLEY, D. S., KOCH, C. J., SLATER, J. M., AND LITTLE, J. B. Overview of radiosensitivity of human tumor cells to low-dose-rate irradiation. *Int J Radiat Oncol Biol Phys* 72 (2008), 909–917.
- [114] WITHERS, H. R. Biologic basis for altered fractionation schemes. *Cancer* 55 (1985), 2086–2095.
- [115] ZHAO, Y., THOMAS, H. D., BATEY, M. A., COWELL, I. G., RICHARDSON, C. J., GRIFFIN, R. J., CALVERT, A. H., NEWELL, D. R., SMITH, G. C. M., AND CURTIN, N. J. Preclinical evaluation of a potent novel dna-dependent protein kinase inhibitor nu7441. *Cancer Res* 66 (2006), 5354–5362.
- [116] ZONG, W.-X., AND THOMPSON, C. B. Necrotic death as a cell fate. *Genes Dev* 20 (2006), 1–15.



## Acknowledgements

I would like to give my sincerest thanks to those who supported me through the work of this thesis.

- Text removed for privacy reasons -



## Curriculum vitae

**Name** Sebastian Haßlacher  
**Date of Birth** removed for privacy reasons  
**Place of Birth** Ravensburg, Germany

### Education

2007 Allgemeine Hochschulreife,  
 Gymnasium Salvatorkolleg Bad Wurzach, Germany  
 2007-2009 Studies of Maths and Physics  
 Technical University of Munich (TUM), Germany  
 2009-2016 Studies of Medicine, Ulm University, Germany  
 2016 Degree in Medicine, Approbation as Medical Doctor  
 2012-2014 Promotionsprogramm "Experimentelle Medizin"  
 International Graduate School of Molecular Medicine, Ulm Germany

### Work

2015-2016 Practical Year at  
 Stauferklinikum Schwäbisch Gmünd, Germany  
 Ngwelezana Hospital, South Africa  
 Kantonsspital Sursee, Switzerland  
 2016-2018 Department of Internal Medicine, Regionalspital Surselva, Switzerland  
 2018- Department of Internal Medicine, Stadtspital Triemli, Switzerland

### Publications

Schneider M, Ströbele S, Nonnenmacher L, Siegelin MD, Tepper M, Stroh S, **Hasslacher S**, Enzenmüller S, Strauss G, Baumann B, Karpel-Massler G., Westhoff MA, Debatin KM, Halatsch ME **A paired comparison between glioblastoma „stem cells“ and differentiated cells.** *Int J Cancer.*, 138:1709-18 (2016)

Nonnenmacher L, **Hasslacher S**, Zimmermann J, Karpel-Massler G, La Ferla-Brühl K, Barry SE, Burster T, Siegelin MD, Brühl O, Halatsch ME, Debatin KM, Westhoff MA. **Cell Death Induction in Cancer Therapy - Past, Present, and Future.** *Crit Rev Oncog.*, 21:253-267 (2016)

Grunert M., Kassubek R., Danz B., Klemenz B., **Hasslacher S.**, Stroh S., Schneelee L., Langhans J., Stöbele S., Barry S.E., Zhou S., Debatin K.M., Westhoff M.A., **Radiation and Brain Tumors: An Overview.** *Critical Reviews in Oncogenesis*, 23: 119-138 (2018)

**Hasslacher S.**, Schneelee L., Stroh S, Langhans J., Zeiler K., Patricia K., Karpel-Massler G., Siegelin M., Schneider M., Zhou S., Grunert M., Halatsch ME., Nonnenmacher L., Debatin K.M., Westhoff M.A. **Inhibition of PI3K signalling inceases the efficiency of radiotherapy in glioblastoma cells.** *International Journal of Oncology*, 53:1881-1896 (2018)